NASA CONTRACTOR REPORT

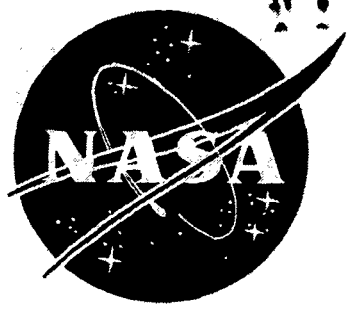

NASA CR–112115

NASA CR–112115

MASTER AGREEMENT TASK ORDER SIX

Analytical Determination of the Effect of Structural Elasticity on Landing Stability of a Version of the Viking Lander

By R.M. Laurenson

Prepared by

MCDONNELL DOUGLAS ASTRONAUTICS COMPANY–EAST
St. Louis, Missouri 63166 (314) 232–0232

for Langley Research Center

NATIONAL AERONAUTICS AND SPACE ADMINISTRATION ● WASHINGTON, D.C. ● AUGUST 1972

NASA CR-112115

MASTER AGREEMENT
TASK ORDER SIX

Analytical Determination Of The Effect Of Structural Elasticity On Landing Stability Of A Version Of The Viking Lander

By R.M. Laurenson

Prepared Under Contract No. NAS 1-8137 by

MCDONNELL DOUGLAS ASTRONAUTICS COMPANY-EAST

Saint Louis, Missouri

for

NATIONAL AERONAUTICS AND SPACE ADMINISTRATION

This Page Intentionally Left Blank.

ABSTRACT

A limited analytical investigation was conducted to assess the effects of structural elasticity on the landing stability of a version of the Viking Lander. Two landing conditions and two lander mass and inertia distributions were considered. The results of this investigation show that the stability-critical surface slopes were lower for an uphill landing than for a downhill landing. In addition, the heavy footpad mass with its corresponding inertia distribution resulted in lower stability-critical ground slopes than were obtained for the light footpad mass and its corresponding inertia distribution. Structural elasticity was observed to have a large effect on the downhill landing stability of the light footpad mass configuration but had a negligible effect on the stability of the other configuration examined. Because of the limited nature of this study, care must be exercised in drawing conclusions from these results relative to the overall stability characteristics of the Viking Lander.

This Page Intentionally Left Blank.

TABLE OF CONTENTS

LIST OF FIGURES

LIST OF FIGURES (CONT.)

LIST OF PAGES

i through x

1 through 70

1.0 INTRODUCTION

During Task Order Six, NASA Contract NAS 1-8137(U), McDonnell Douglas Astronautics Company - East conducted an analytical investigation to assess the effects of the Viking Lander's structural elasticity on the vehicle's landing stability. Results of this stability investigation are presented in this document.

The Landing Loads and Motions Program developed during Task Order Five, Reference 1, was used for this study. Data defining the Viking Lander structural configuration were supplied by NASA Langley Research Center, Reference 2. Viking Lander center body flexibility information, frequencies and mode shapes, was supplied by Martin Marietta Corporation, Reference 3.

Two landing conditions and two assumed lander mass and inertia distributions were considered during these studies. For all of these cases, the critical ground slope resulting in lander instability for both a rigid and flexible lander was determined. In addition, the effect on stability of the nonsymmetric nature of both lander inertia properties and center body mode shapes was investigated.

The initial conditions for the two landing conditions investigated were similar. The major difference between the two was the direction of the initial lander horizontal velocity. For the Downhill Landing this velocity was directed away from the slope of the landing surface. This initial horizontal velocity was directed into the landing surface slope for the Uphill Landing.

The two lander mass and inertia distributions differed by the relative inertia properties of the lander's footpads and center body employed in the Viking Lander idealization. For the Full Footpad mass distribution, the center body and footpad mass and inertias as defined in Reference 2 were employed. In the Light Footpad mass distribution it was assumed that only five percent of the footpad mass was effective at the footpad pivot point. The remaining footpad mass and inertia contributions about the center of gravity were included with the center body properties. Note that both of these mass distributions resulted in the same total Viking Lander mass and inertia characteristics before stroking of the legs.

This Page Intentionally Left Blank.

2.0 SUMMARY

During Task Order Six a number of analytical landing studies were conducted to assess the effects of structural elasticity on the landing stability of the Viking Lander. It was shown that Viking Lander structural elasticity can have a large effect on landing stability. For a Downhill Landing with the Light Footpad mass distribution, the inclusion of elasticity resulted in a six degree reduction in the critical ground slope for landing stability when compared with rigid body stability. However, for the remaining cases investigated during Task Order Six, the inclusion of structural elasticity had negligible effect on Viking Lander stability.

A number of additional aspects of Viking Lander stability were observed during Task Order Six. For instance, these study results showed that Viking Lander stability-critical ground slopes were lower for the Uphill Landing when compared to the Downhill Landing. This trend was true whether or not the effects of structural elasticity were included in the lander's idealization.

In addition, the Full Footpad mass and inertia idealization resulted in lower stability-critical ground slopes than did the Light Footpad mass distribution. For instance, the worst stability case for the Light Footpad mass distribution resulted in a 22 degree ground slope required for a stable landing while the comparable result for the Full Footpad distribution was 14 degrees.

3.0 VIKING LANDER IDEALIZATION

The Viking Lander idealization employed throughout the Task Order Six landing stability studies was based on data supplied in References 2 and 3. Geometric data (coordinates of strut attach points, etc.), strut load stroke curves, footpad idealization, and soil properties remained constant during this investigation. Two lander mass and inertia distributions, referred to as the Full Footpad and Light Footpad mass distributions, were considered. These distributions are defined in Section 3.2. The Viking Lander modal data (center body frequencies and mode shapes) used to represent lander structural flexibility are discussed in Section 3.3. Plots of these mode shapes are presented in Appendix A.

The general arrangement of the Viking Lander is shown in Figure 3-1. The lander is composed of a center body and three legs. The vehicle's scientific payload, power supplies, terminal descent engines, etc., are mounted on the center body structure. Each leg is made up of a main strut and two drag struts. The main strut contains an energy absorption system of stacked honeycomb cartridges. The drag struts are stiff members which stabilize the legs. As shown in Figure 3-2, a load alleviator is located at the center body end of each drag strut. This load alleviator bends plastically and thus limits the loads transmitted to the center body structure by the drag struts. At the base of each leg is a footpad which makes actual contact with the landing surface.

The Landing Loads and Motions Program developed during Task Order Five, Reference 1, for the prediction of the landing dynamics of legged landers, was used for the Task Order Six stability studies. The capabilities and options of this program influenced many of the decisions made in arriving at the idealization of the Viking Lander. For this reason a brief description of the program is presented below. Complete documentation of the Landing Loads and Motions Program may be found in Reference 1.

With the Landing Loads and Motions Program, the lander center body may be idealized as either a rigid body or the effects of a flexible structure may be included. The flexible center body effects are obtained by the superposition of elastic motions, represented by a number of free-free vibratory modes, on the rigid body motion. From one to five of these modes may be included in the analysis.

The legs for a given lander configuration consist of a main strut and two drag struts which have pinned ends; thus, no moments or torques may be introduced at their ends. Both the main strut and drag struts are capable of carrying tension and compression loads and may possess velocity dependent force characteristics, elastic-plastic load stroke characteristics, or a combination of the two. Five plastic load levels are available in both tension and compression for all of the landing gear struts. The load stroke characteristics of all main struts in a given lander configuration are the same. Likewise, these characteristics for all the drag struts are the same, however, they may be different than the main struts.

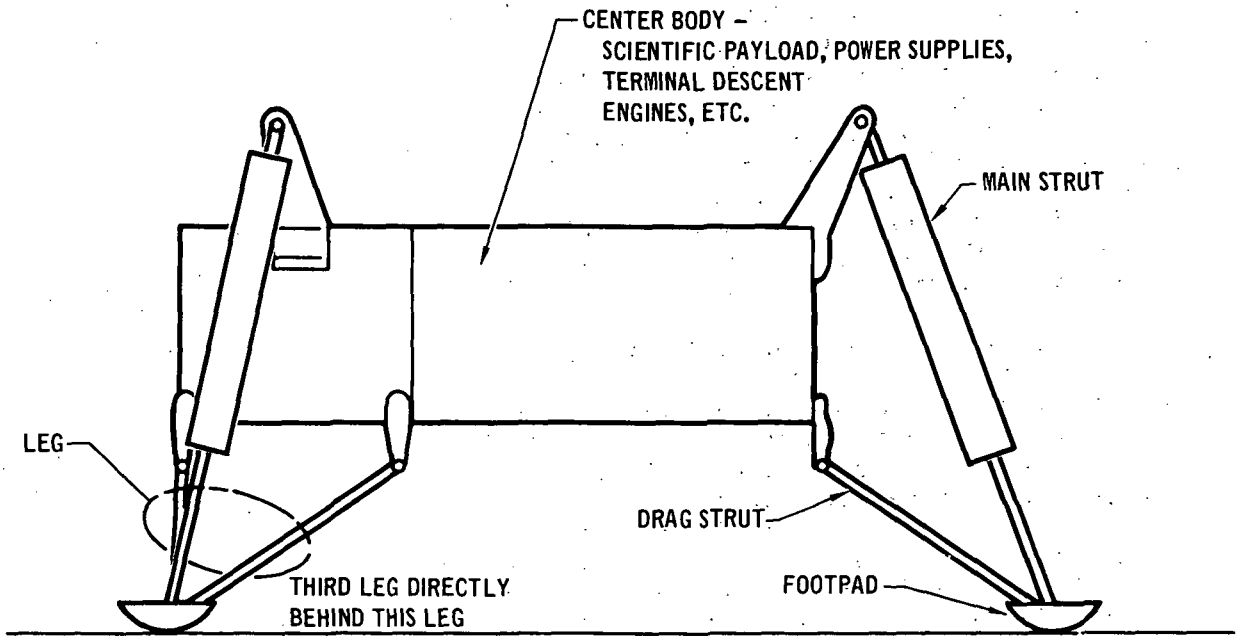

FIGURE 3–1 GENERAL ARRANGEMENT OF THE VIKING LANDER

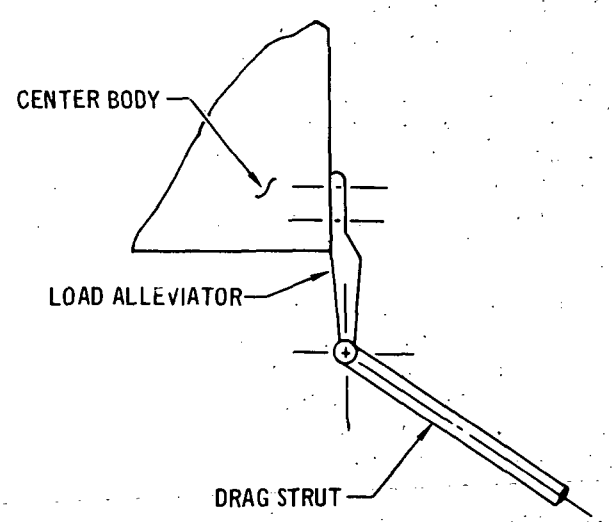

FIGURE 3–2 VIKING LANDER DRAG STRUT LOAD ALLEVIATOR ATTACHMENT

Each footpad is represented as a single mass with three rigid body translational degrees of freedom. One degree of freedom is normal to the landing surface and the other two are in the plane of the landing surface. On an optional basis, a plastic load attenuation material, with up to three crush levels, may be located on the bottom of each footpad. For footpads whose equations of motion are not being integrated, the associated gears are assumed to be extensions of the center body structure and their inertia effects are included in the center body equations of motion.

Two soil mechanics routines are available for studying the footpad-soil interaction phenomenon. The Primary Soil Mechanics option is similar to the footpad-soil interaction analysis developed during the Lunar Module Soil Mechanics Study. In this case, the soil is represented in terms of a number of semiempirical relationships. The Secondary Soil Mechanics method determines the soil force through a simple elastic-plastic relationship between soil pressure and depth of soil penetration in conjunction with a coefficient of friction.

3.1 Structural Configuration

Figure 3-3 defines the coordinates of all the leg strut attach points and the footpad pivot points relative to the center body center of gravity. The coordinate system shown in this figure corresponds to the coordinate system defined in the NASA data transmittal letter, Reference 2. It has been assumed that the drag strut loads are applied to the center body at the drag strut end of the load alleviators, Figure 3-2. The load carrying characteristics of the load alleviator have been incorporated in the drag strut load stroke relationship.

Sketches of the actual footpad and the footpad idealization used in the landing studies are shown in Figure 3-4. The Secondary Soil Mechanics routine, Reference 1, was employed throughout the investigation to simulate a stiff (hard) landing surface using the following soil parameters:

soil elasticity constant = 3.257×10^8 N/m^3

maximum soil pressure = 9.653×10^7 N/m^2

coefficient of friction = 1.0

It was assumed that the effective drag strut load stroke curve was the series combination of the load alleviator and drag strut load stroke characteristics. This nonlinear load stroke relationship was represented by a series of straight line segments to be compatible with the Landing Loads and Motions Program. Thus, the load alleviator load stroke curve shown in Figure 3-5 was divided into a number of straight line segments. The spring rate of each of these straight lines acting in series with the spring rate of the drag strut (2.872×10^7 N/m) resulted in the effective drag strut load stroke curve shown in Figure 3-6. The effective drag strut load stroke curve

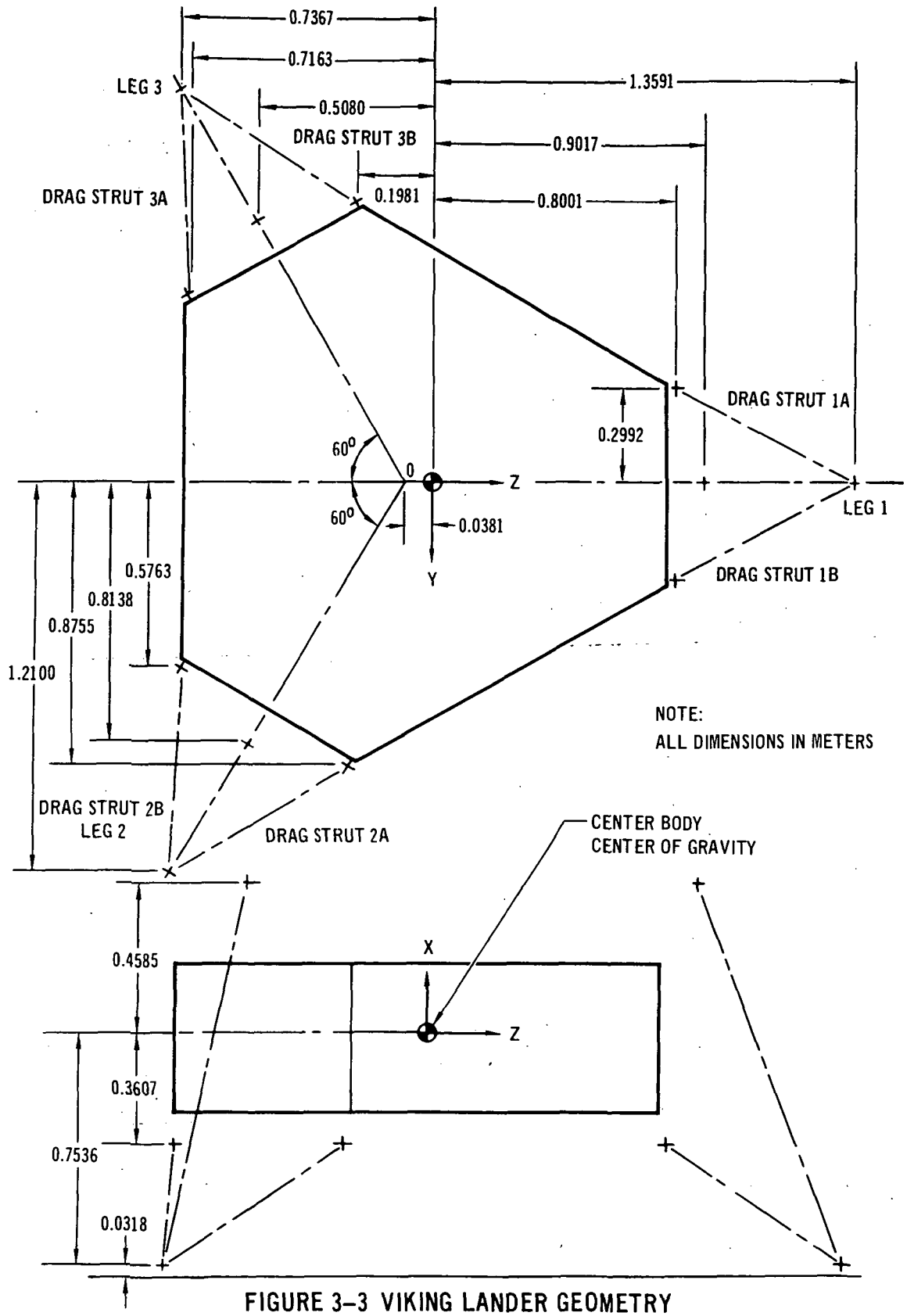

FIGURE 3–3 VIKING LANDER GEOMETRY

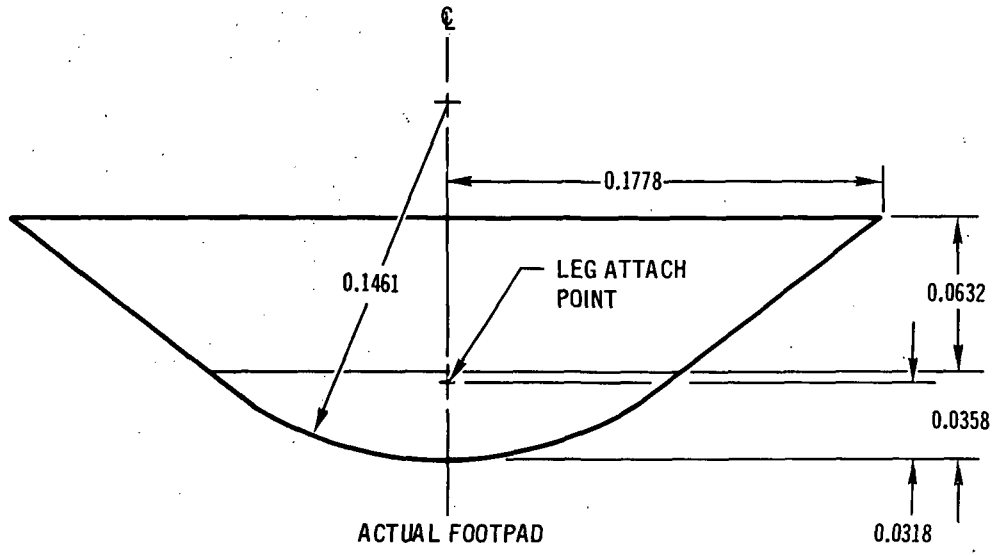

ALL DIMENSIONS IN METERS

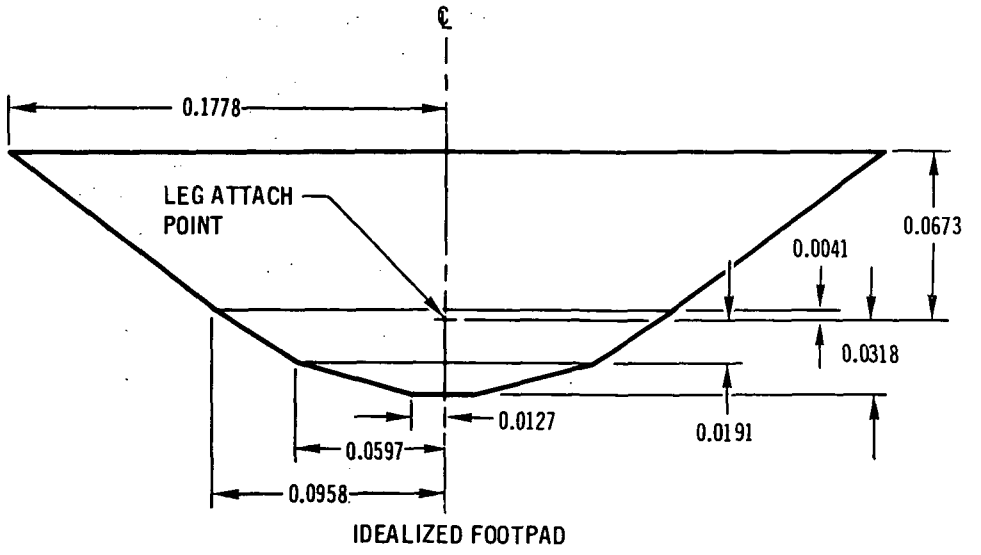

FIGURE 3–4 VIKING LANDER FOOTPAD IDEALIZATION

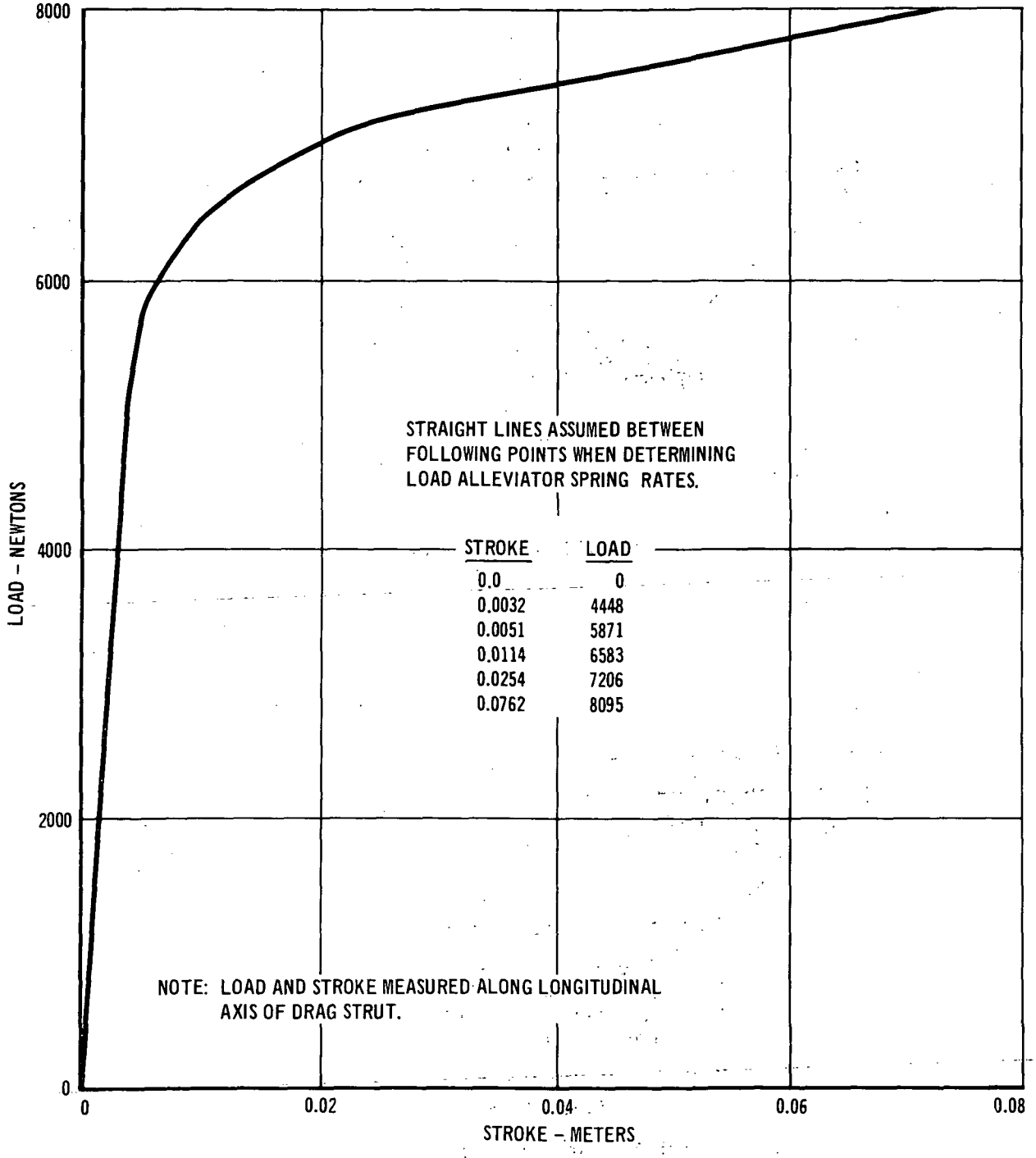

FIGURE 3-5 LOAD STROKE CURVE FOR VIKING LANDER LOAD ALLEVIATOR

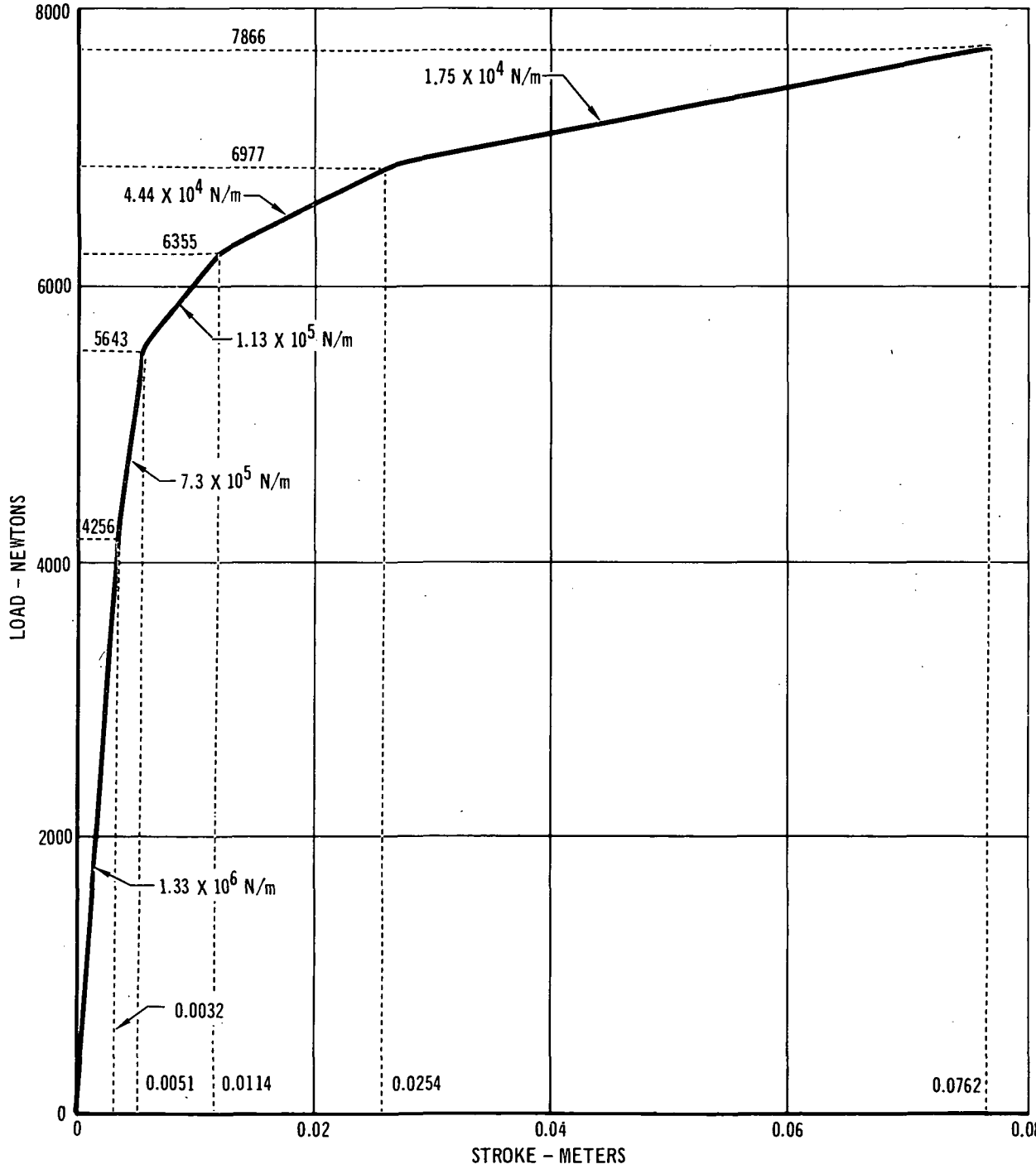

FIGURE 3-6 EFFECTIVE DRAG STRUT LOAD STROKE CURVE

shown in this figure was employed for both tension and compression loading. The characteristics of the load alleviator required some modifications to the drag strut idealization in the Landing Loads and Motions Program. These modifications are discussed in Appendix B.

The load stroke characteristics of the Viking Lander main strut are governed by the crush levels of the honeycomb cartridges housed within the strut. Based on data supplied in Reference 2, the main strut load stroke relationship employed during Task Order Six is given in Figure 3-7.

3.2 Mass and Inertia Distributions

The two lander mass and inertia distributions employed during Task Order Six are summarized in Figure 3-8. The Full Footpad mass distribution used the footpad mass and center body mass and inertias given in Reference 2. In this distribution the mass of each footpad was 3.384 kilograms and the mass of the center body was 565.4 kilograms.

The Light Footpad mass distribution assumed a majority of the footpad mass was associated with the center body mass and inertia properties. This distribution was investigated to permit correlation with a program being used at NASA Langley Research Center which is limited to massless footpads and relates the total vehicle mass and inertias to the center body mass and inertia properties. In the Light Footpad mass distribution the assumed footpad mass was 0.175 kilograms. The difference between this mass and the actual mass for each footpad (3.384-0.175 kilograms) was included in the center body mass. In addition, the moments of inertia of this difference in mass, 3.209 kilograms for each footpad, about the center body center of gravity, was included in the center body moments of inertia.

3.3 Mode Set Selection Criteria

Four sets of Viking Lander center body modal data, each containing five modes, were selected to represent the effects of structural flexibility for the Task Order Six landing stability studies. A summary of these four mode sets is presented in Figure 3-9. Plots of the mode shapes for these modes are presented in Appendix A.

The criteria for selecting the modes to be included in Mode Sets A, B, and C, Figure 3-9, were the same. The deflection pattern (mode shape) for each Viking Lander mode was reviewed and those modes that did not experience significant modal deformation at the landing gear strut attach points were eliminated from further consideration. It was assumed that modes having at least one strut attach point with a modal deflection of 10 percent or more of the maximum deflection amplitude in that mode, would be used in the landing studies. Mode Set A is made up of the five lowest frequency modes meeting this condition; Mode Set B is made up of the next five lowest frequency modes, etc.

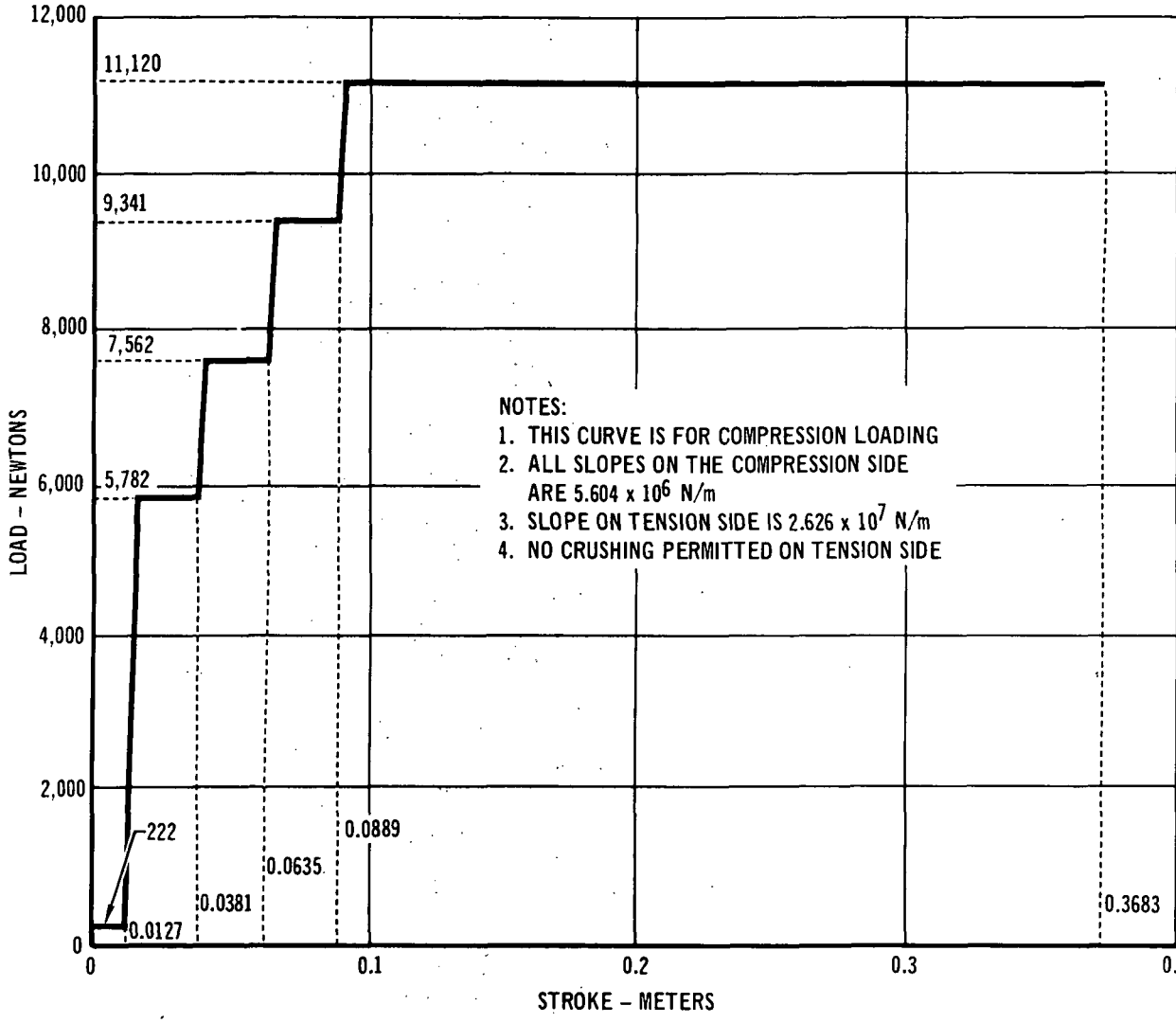

FIGURE 3–7 VIKING LANDER MAIN STRUT LOAD STROKE CURVE

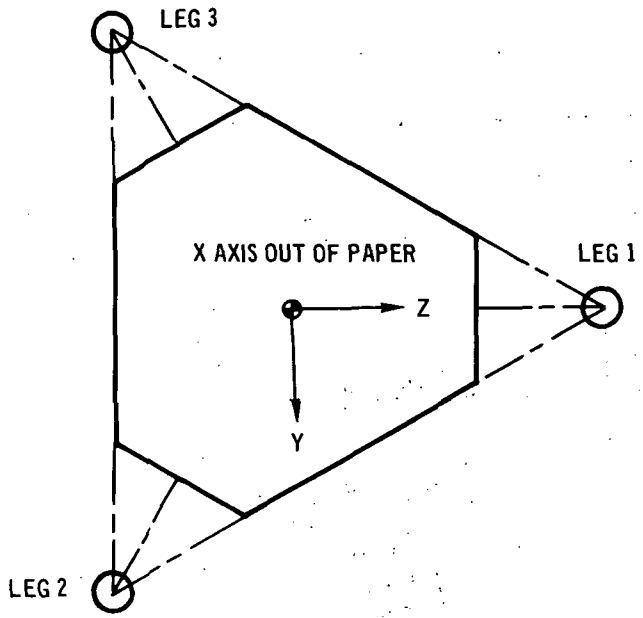

CENTER BODY – M = 565.4 KILOGRAMS

I_{xx} = 292.7 kg–m^2

I_{yy} = 147.0 kg–m^2

I_{zz} = 191.7 kg–m^2

$I_{xy} = I_{xz} = I_{yz} = 0$

FOOTPAD – m = 3.384 KILOGRAMS PER FOOTPAD

Full Footpad Mass Distribution

CENTER BODY – M = 575.0 KILOGRAMS

I_{xx} = 311.5 kg–m^2

I_{yy} = 161.9 kg–m^2

I_{zz} = 206.6 kg–m^2

$I_{xy} = I_{xz} = I_{yz} = 0$

FOOTPAD – m = 0.175 KILOGRAMS PER FOOTPAD

Light Footpad Mass Distribution

FIGURE 3–8 VIKING LANDER MASS AND INERTIA DISTRIBUTIONS

The modes contained in Mode Set D were drawn from modes included in the other three sets. Not only did the modes contained in this set experience significant modal deflection at the leg attach points, but the pattern of the deflection shape was considered. For an initial impact of footpad three and the two landing conditions considered during Task Order Six, nearly symmetrical landings result about a line through footpad three and point O, Figure 3-3. Referring to the mode shape plots in Appendix A, Mode Set D is made up of those modes having symmetry about this line. For an initial impact of footpad three, the nonsymmetric modes will not be excited by the nearly symmetric strut load patterns resulting during the two landing conditions investigated.

MODE SET A					
ELASTIC MODE NUMBER	1	5	6	7	18
FREQUENCY - H_z	12.03	15.88	15.95	23.86	41.74
MODE SET B					
ELASTIC MODE NUMBER	21	22	23	24	25
FREQUENCY - H_z	45.43	45.99	47.11	50.21	51.86
MODE SET C					
ELASTIC MODE NUMBER	26	27	28	29	31
FREQUENCY - H_z	53.07	54.86	56.24	60.61	67.95
MODE SET D					
ELASTIC MODE NUMBER	5	7	23	24	26
FREQUENCY - H_z	15.88	23.86	47.11	50.21	53.07

FIGURE 3-9 SUMMARY OF VIKING LANDER MODAL DATA

4.0 RESULTS OF VIKING LANDER STABILITY STUDIES

Effects of structural elasticity on Viking Lander stability have been established for two landing conditions and two lander mass and inertia distributions. This was accomplished by comparing stability of the lander including elasticity effects to the stability obtained assuming a rigid body. Initial conditions for the two landings, Downhill and Uphill Landings, are shown in Figure 4-1. These landing conditions are similar with the major difference being in the direction of the lander's initial horizontal velocity. For the Downhill Landing this velocity is directed away from the slope. In the Uphill Landing the horizontal velocity is directed into the ground slope. In addition, the Downhill Landing had an initial pitch rate of 5 degrees/second while the Uphill Landing had no initial pitch rate. The two mass and inertia distributions, referred to as the Light Footpad and Full Footpad mass distributions, are defined in Figure 3-8, Section 3.2.

In these investigations, lander stability is expressed in terms of the ground slope angle which results in an unstable landing. For each configuration considered, all parameters were held constant while the ground slope was varied until the stability boundary was determined within a tolerance of one degree on the critical slope. Therefore, the slope angle resulting in a stable landing did not differ by more than one degree from the slope angle resulting in an unstable landing.

In the following sections, rigid body and elastic body stability results are presented for each lander mass and inertia distribution. Discussion of these stability studies addresses the combined results of all the cases investigated and is presented in Section 5.0. The discussion of these combined results allows conclusions to be drawn from the complete Task Order Six study results.

4.1 Stability With Light Footpad Mass Distribution

Stability of the Viking Lander employing the Light Footpad mass distribution was determined for both landing conditions, Figure 4-1, with an initial impact of footpad three. This orientation of the lander was selected so that the offset center of gravity was located the maximum distance from the footpad making initial contact with the landing surface (see Figure 3-3). Note that an initial impact of footpad two would have given the same result.

Landing stability results for the Light Footpad mass distribution are summarized in Figure 4-2. Four mode sets, summarized in Figure 3-9, Section 3.3, were employed in representing structural flexibility effects. As indicated in Figure 4-2, for the two landing conditions investigated, the inclusion of structural flexibility can have a marked effect on stability of the Viking Lander. It is interesting to note that the low frequency modes are the most important in assessing the effects of structural flexibility on landing stability. Secondly, for the two landing conditions investigated, flexibility greatly affected the results for the Downhill Landing, but made no significant difference for Uphill Landing.

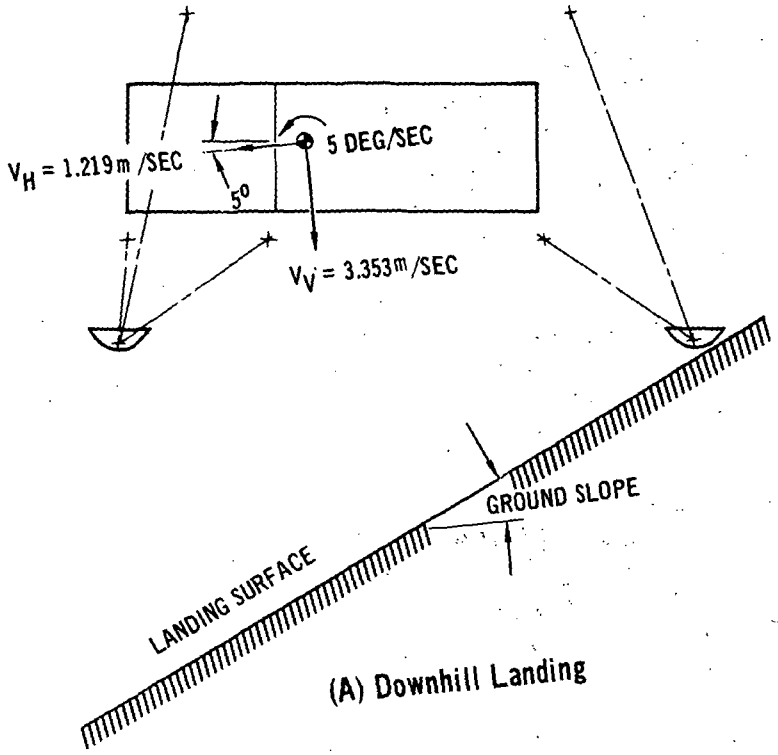

(A) Downhill Landing

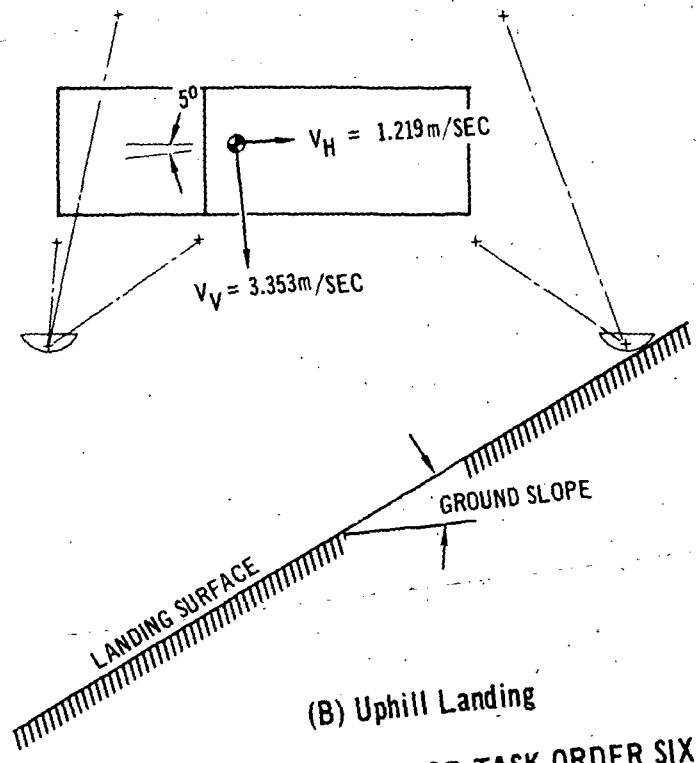

(B) Uphill Landing

FIGURE 4-1 INITIAL CONDITIONS FOR TASK ORDER SIX LANDING CASES

MODE SET	MODE SET FREQUENCY RANGE – Hz	CRITICAL GROUND SLOPE–DEG DOWNHILL LANDING		CRITICAL GROUND SLOPE–DEG UPHILL LANDING	
		STABLE	UNSTABLE	STABLE	UNSTABLE
RIGID BODY	–	30	31	22	23
A	12.03–41.74	24	25	22	23
B	45.43–51.86	25	26	23	24
C	53.07–67.95	27	28	22	23
D	15.88–53.07	24	25	23	24

NOTE: THESE RESULTS ARE ALL FOR AN INITIAL IMPACT OF FOOTPAD THREE

FIGURE 4–2 STABILITY RESULTS FOR LIGHT FOOTPAD MASS DISTRIBUTION

4.2 Stability With Full Footpad Mass Distribution

To assess effects of the nonsymmetric nature of both the Viking Lander inertia properties and mode shapes, a second phase of the stability investigation was conducted. Stability was determined for an initial impact of footpad three and both landing conditions shown in Figure 4-1 with the Full Footpad mass distribution. This was followed by the stability determination for an initial impact of footpad one and then for an initial impact of footpad two.

Both rigid body and elastic body (Mode Set A) stability-critical ground slopes were obtained in all these cases and are summarized in Figure 4-3. As indicated in this figure, for the rigid body cases, the nonsymmetric inertia properties had a significant effect on the landing stability. For the same landing condition, as much as a five degree change in the critical ground slope was obtained. At these lower critical ground slopes, the addition of center body flexibility had an insignificant effect compared to the results noted with the Light Footpad mass distribution.

LANDER ORIENTATION	CRITICAL GROUND SLOPE – DEG DOWNHILL LANDING		CRITICAL GROUND SLOPE – DEG UPHILL LANDING	
	STABLE	UNSTABLE	STABLE	UNSTABLE
LEG 1 FIRST				
RIGID BODY	22	23	19	20
ELASTIC BODY	22	23	19	20
LEG 2 FIRST				
RIGID BODY	19	20	14	15
ELASTIC BODY	19	20	14	15
LEG 3 FIRST				
RIGID BODY	19	20	14	15
ELASTIC BODY	19	20	14	15

NOTE: ELASTIC BODY RESULTS ARE FOR MODE SET A

FIGURE 4–3 STABILITY RESULTS FOR FULL FOOTPAD MASS DISTRIBUTION

5.0 DISCUSSION OF VIKING LANDER STABILITY STUDY RESULTS

A summary of the results of the Task Order Six landing stability studies is presented in Section 4.0. Following are a number of observations which may be made concerning these results.

1. For both lander mass distributions and either rigid or elastic body lander representation, the Uphill Landing resulted in the lowest ground slope angle for a stable landing.

2. For a particular set of initial conditions, the Full Footpad mass distribution was less stable than the Light Footpad mass distribution.

3. For the Full Footpad mass distribution and a given set of initial conditions, the lander was less stable with an initial impact of footpad two or three than with an initial impact of footpad one.

4. For the Light Footpad mass distribution and a Downhill Landing, structural flexibility had a large effect on lander stability. Inclusion of flexibility had negligible effect on stability for the remaining combinations of lander mass distributions and sets of landing conditions.

The above points are fully discussed in the following sections. In a number of cases, these stability results are interpreted in terms of the lander's stability angle discussed below.

To determine the stability of a lander configuration, the "plane of lander motion," as shown in Figure 5-1, is defined. This plane is defined by the gravity vector, $\bar{g}$, and the resultant translational velocity, $\bar{V}_{cg}$, of the lander's center of gravity. The case encountered during Task Order Six, with two footpads astride the plane of lander motion, is shown in Figure 5-1. In this case, the vector $\bar{L}$, extending from the lander center of gravity to the intersection point of a line between these two footpads and the plane of lander motion is obtained. The stability angle, S, is the angle between $\bar{L}$ and $\bar{g}$, and is defined as:

$$S = \text{Cos}^{-1}\left(\frac{(\bar{L}.\bar{g})}{|\bar{L}|\,|\bar{g}|}\right)$$

As long as S is positive, the lander is considered to be stable. When S passes through zero, the lander is said to be experiencing pitch instability. For a negative S, the weight of the lander causes a destabilizing moment about the footpads.

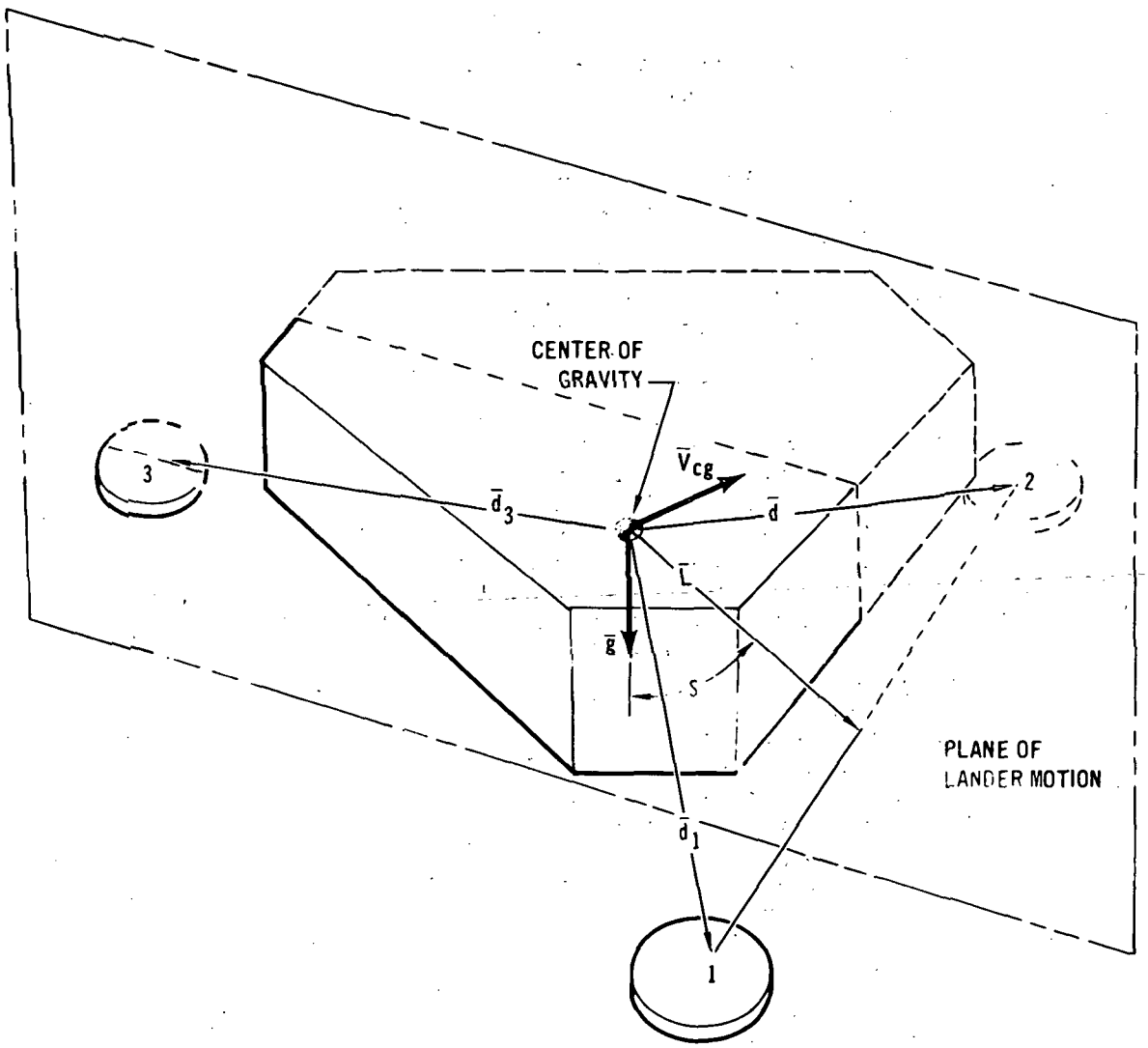

FIGURE 5–1 LANDER STABILITY ANGLE

5.1 Stability Comparison for Different Initial Conditions

In all cases investigated during Task Order Six, the initial conditions associated with the Uphill Landing resulted in a less stable landing condition than for a Downhill Landing. This is to be expected since the resultant initial center of gravity velocity, Figure 5-2, is more nearly directed through the leg whose footpad makes initial impact for the Uphill Landing condition. Therefore, in the Uphill Landing, much larger loads are developed in the struts of this leg and the resulting lander pitch velocity is higher than for a Downhill Landing.

For a 30 degree ground slope, this difference in pitch velocity between an Uphill and Downhill Landing is shown in Figure 5-3. In this case, the Light Footpad mass distribution was employed. For these conditions, the Downhill Landing is stable while the Uphill Landing is unstable.

5.2 Stability Comparison for Different Lander Mass Distributions

The Viking Lander represented by the Full Footpad mass distribution was less stable than the Light Footpad mass distribution for both sets of initial conditions investigated. To illustrate this point, consider an Uphill Landing with an initial impact of footpad three on a 22 degree ground slope. As shown in Figure 5-4, this results in a stable landing for the Light Footpad mass distribution and an unstable landing for the Full Footpad mass distribution.

For these two cases, a comparison of strut loads for the leg whose footpad makes initial impact is presented in Figures 5-5 and 5-6. Of importance to lander stability is the somewhat higher drag strut loads, Figure 5-6, acting over a longer period of time for the Full Footpad mass distribution. These higher loads result in a higher destabilizing moment acting for a longer time, causing the Full Footpad mass distribution to experience a higher pitching velocity, Figure 5-7, when the lander rebounds from the landing surface. Upon impact of the downhill legs, this higher pitch velocity results in overturning of the lander.

The drag strut loads acting for a longer time with the Full Footpad mass distribution is to be expected. Since the load levels in the leg struts are of the same order of magnitude for the two mass distributions, the resulting footpad acceleration is dependent on the magnitude of the footpad mass. The heavier footpad in the Full Footpad mass distribution does not experience as high accelerations as does the footpad in the Light Footpad mass distribution. Therefore, following impact, the light footpad moves more rapidly up the slope, thus limiting the stroke, and consequently the loads, in the drag struts.

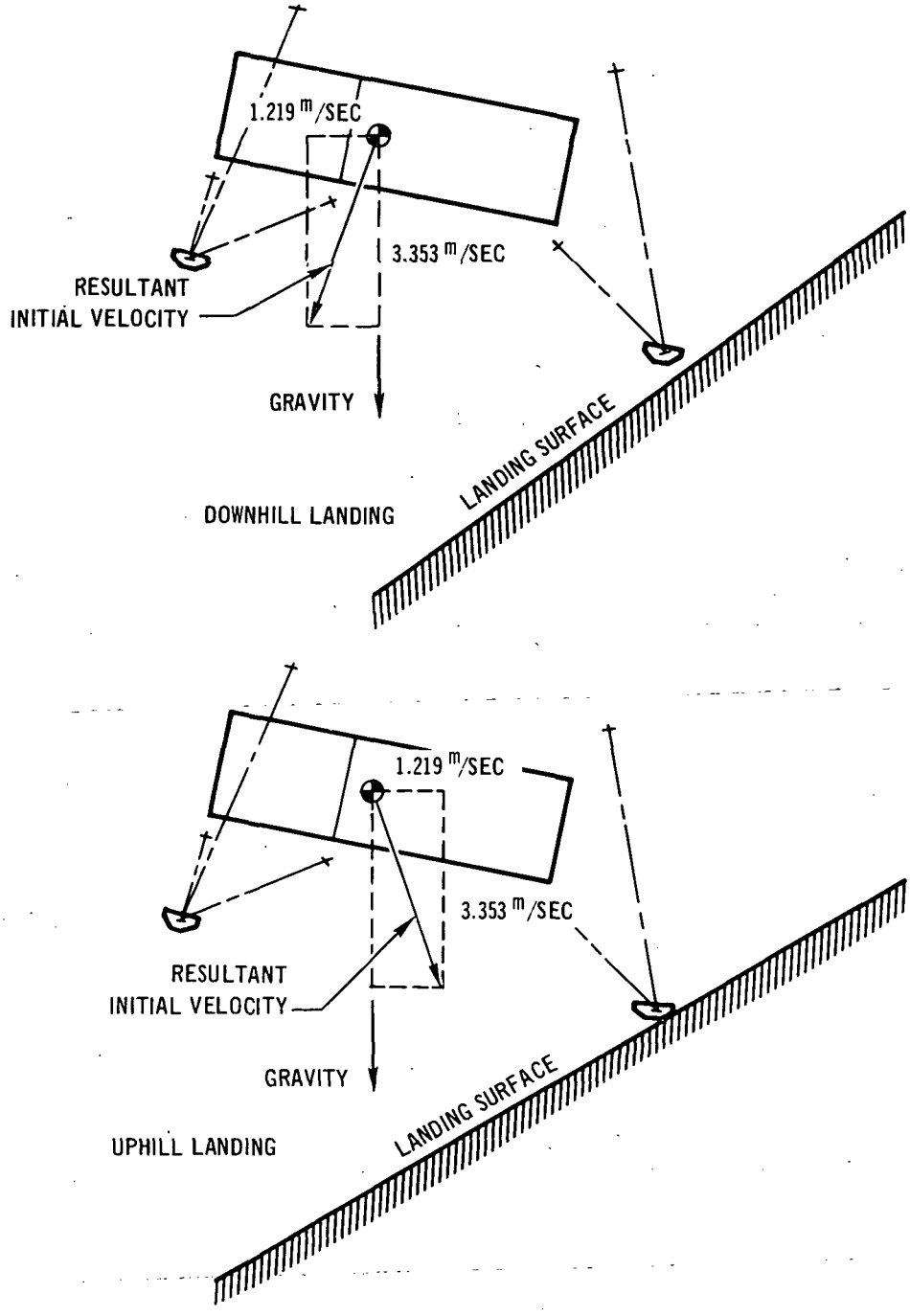

FIGURE 5–2 RESULTANT INITIAL VELOCITY VECTOR COMPARISON FOR UPHILL AND DOWNHILL LANDINGS

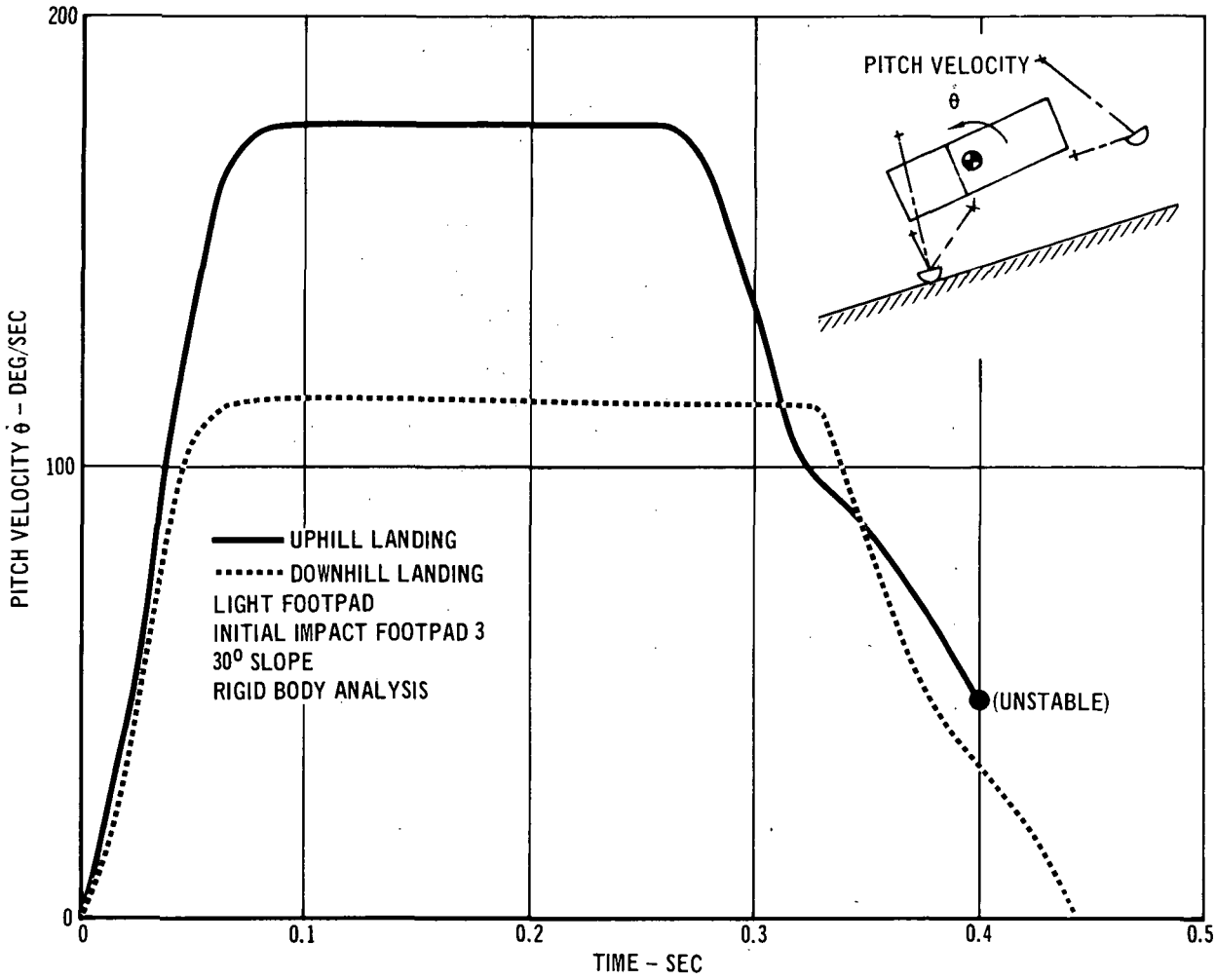

FIGURE 5–3 COMPARISON OF PITCH VELOCITY FOR UPHILL AND DOWNHILL LANDINGS

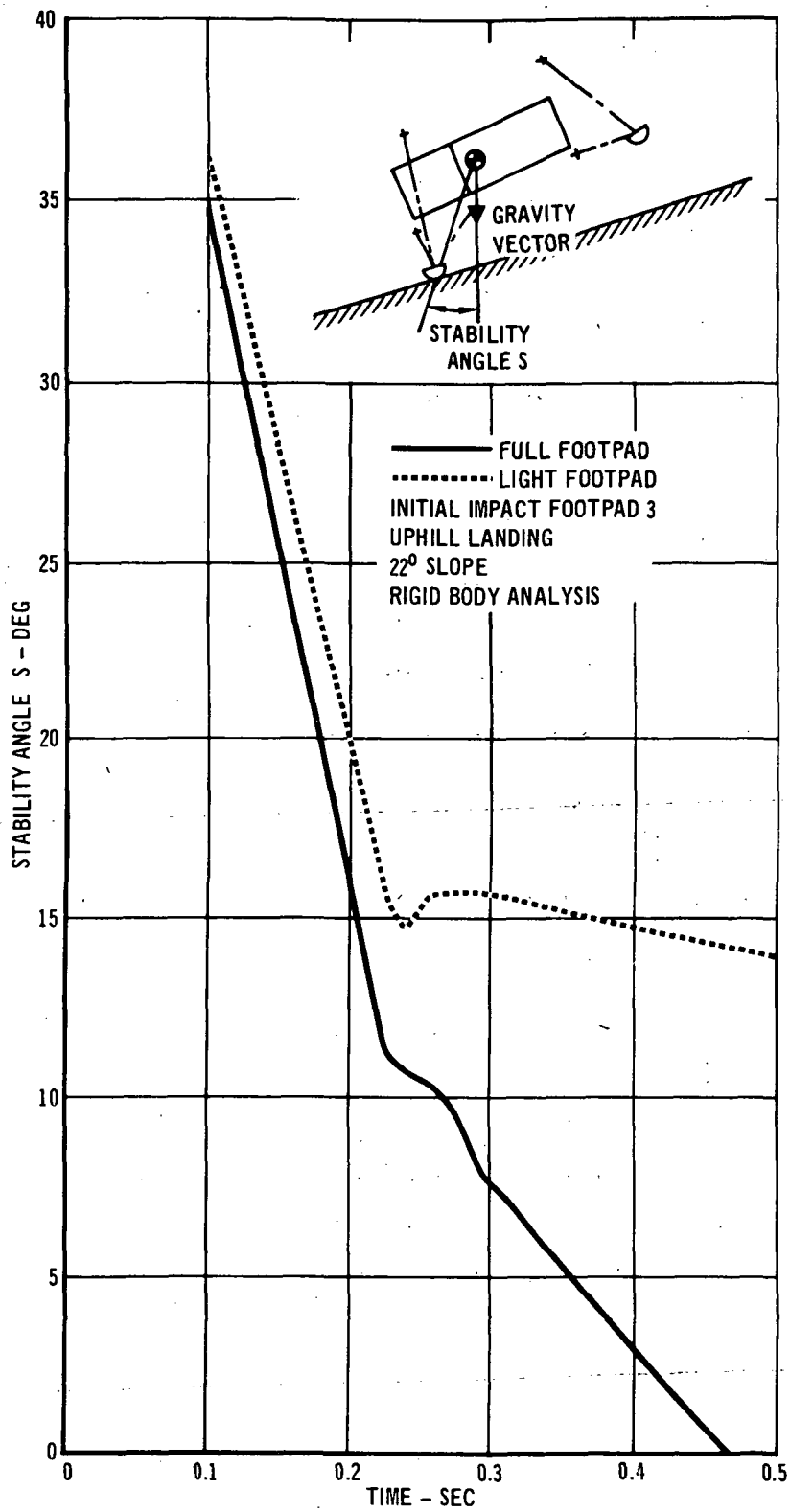

FIGURE 5–4 STABILITY ANGLE COMPARISON FOR DIFFERENT LANDER MASS DISTRIBUTIONS

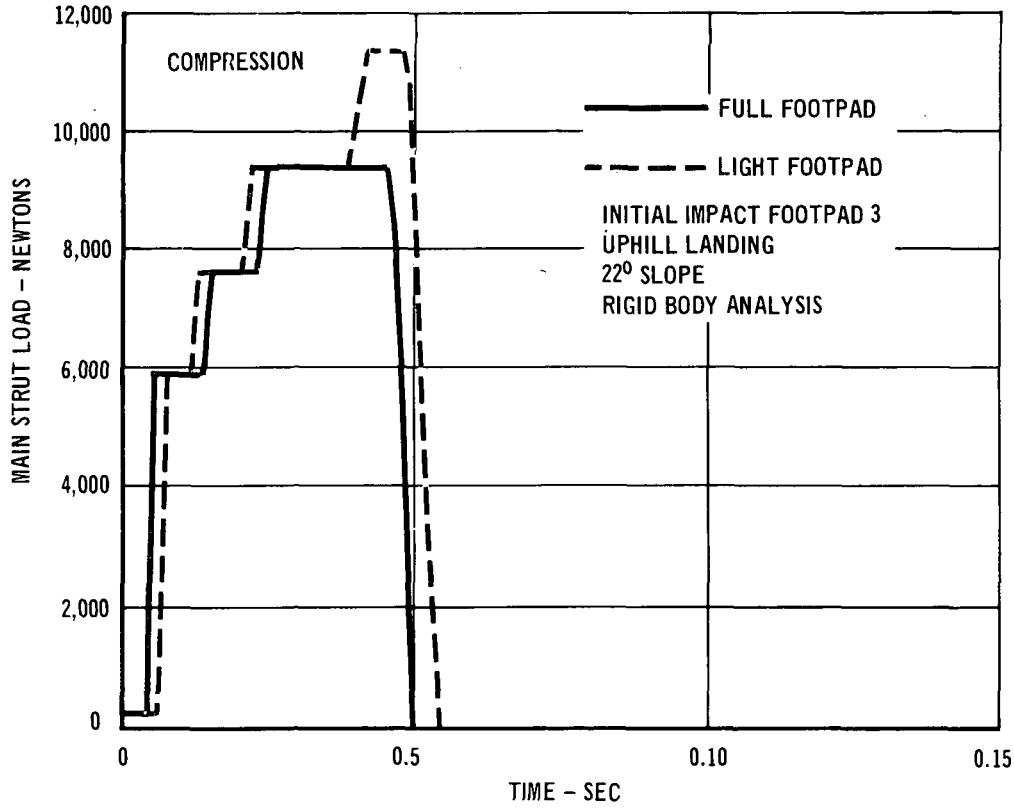

FIGURE 5–5 LEG 3 MAIN STRUT LOAD COMPARISON FOR DIFFERENT LANDER MASS DISTRIBUTIONS

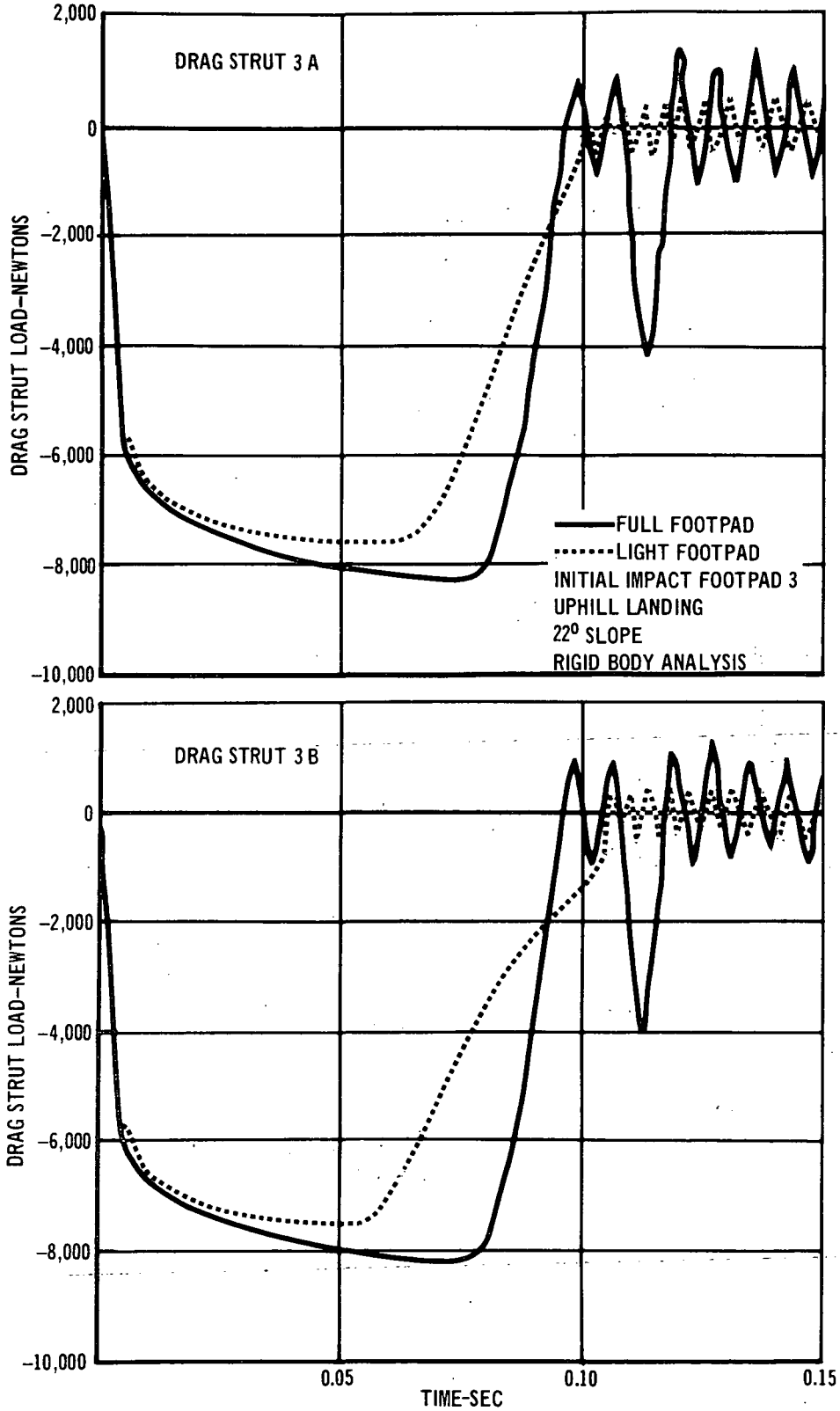

FIGURE 5–6 LEG 3 DRAG STRUT LOAD COMPARISONS FOR DIFFERENT LANDER MASS DISTRIBUTIONS

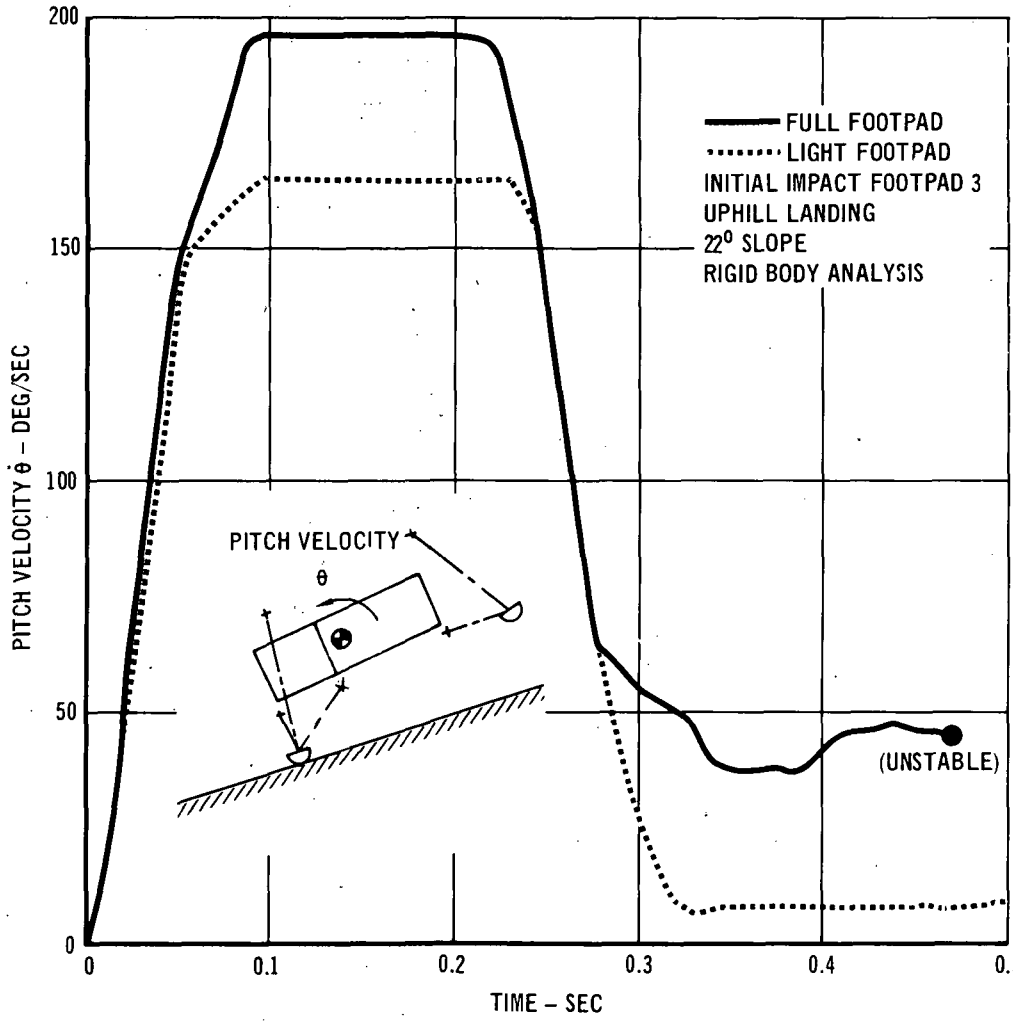

FIGURE 5–7 PITCH VELOCITY COMPARISONS FOR DIFFERENT LANDER MASS DISTRIBUTIONS

5.3 Stability Comparison for Initial Impact on Different Footpads

As summarized in Figure 4-3, all landings in which footpad one impacted initially were the most stable for both Uphill and Downhill Landings. The less stable landings which occurred for initial impacts of footpad two or three may be attributed to the nonsymmetric nature of the Viking Lander. These nonsymmetric properties are due to the offset lander center of gravity, the nonsymmetric lander moments of inertia, and the nonsymmetric nature of the lander's mode shapes.

For instance, with an initial impact of footpad three, the predominant pitching motion is about the Y* axis shown in Figure 5-8. For an initial impact of footpad one, the pitching motion is about the Y axis. The inertia properties influencing motion about the Y* axis are not the same as the properties governing motion about the Y axis. This is illustrated in Figure 5-8, where the Viking Lander inertia properties are expressed in both the X, Y, Z and X*, Y*, Z* coordinate systems.

For an initial impact of footpad one, the motion is symmetric and the downhill footpads impact at the same time. However, for an initial impact of footpad three (or footpad two), the motion is not symmetric, due to the offset center of gravity and the nonsymmetric characteristics of the inertias influencing motion about the Y* axis. Thus, for an initial impact of footpad three, the downhill footpads do not impact simultaneously. One downhill footpad comes in contact with the landing surface and rebounds as the second footpad comes in contact. These downhill footpads continue to "walk" down the hill and the two legs are not fully effective in counteracting the rotational motion of the lander. This is illustrated in Figure 5-9 by a continual decrease in the stability angle to the point of instability for an initial impact of footpad three as compared to that for an initial impact of footpad one.

It should be noted that this dependence of landing stability on sequence of footpad impacts has been verified two ways. Stability of the lander represented by the inertia properties expressed in the X, Y, Z coordinate system, Figure 5-8, and with the proper angular orientation for an initial impact of footpad three, was determined. These results compared well with the stability obtained for a lander represented by the transformed inertia properties expressed in the X*, Y*, Z* coordinate system and with an initial impact occurring on footpad three.

Results for different initial footpad impacts, when lander flexibility is included, are discussed in Section 5.4. For the conditions studied, it appears that the most important factors in determining the effect of the order of footpad impacts are the rigid body inertia properties of the lander.

5.4 Comparison of Rigid and Elastic Body Stability

Comparisons of all rigid body and elastic body landings investigated during the Task Order Six study are presented as time histories of stability

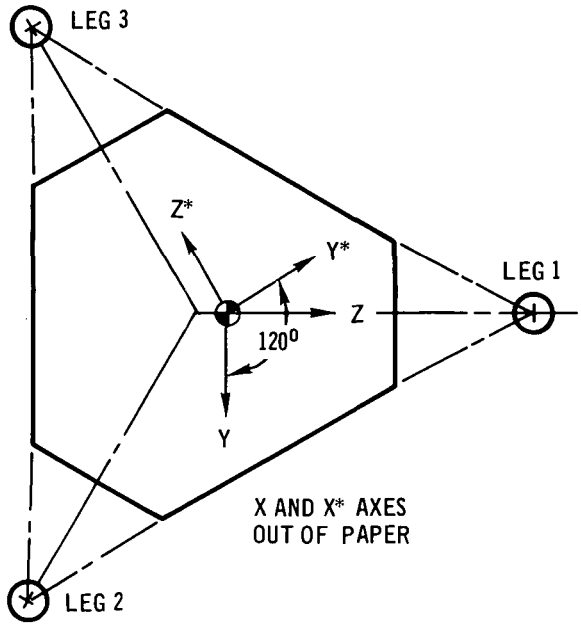

INERTIA PROPERTIES IN X,Y,Z COORDINATE SYSTEM

$I_{xx} = 292.7 \text{ kg-m}^2$
$I_{yy} = 147.0 \text{ kg-m}^2$
$I_{zz} = 191.7 \text{ kg-m}^2$
$I_{xy} = I_{xz} = I_{yz} = 0$

ABOVE VALUES ARE FOR THE FULL FOOTPAD MASS DISTRIBUTION

TRANSFORMATION TO EXPRESS INERTIA PROPERTIES IN X*, Y*, Z* COORDINATE SYSTEM, REFERENCE 4.

$$[I^*] = [T][I][T]^T$$

WHERE [I] IS THE MATRIX OF INERTIAS IN X,Y, Z COORDINATE SYSTEM AND THE TRANSFORMATION MATRIX[T] IS GIVEN AS FOLLOWS:

$$[T] = \begin{bmatrix} 1 & 0 & 0 \\ 0 & \text{COS } 120 & \text{SIN } 120 \\ 0 & -\text{SIN } 120 & \text{COS } 120 \end{bmatrix}$$

THUS THE VIKING LANDER'S INERTIA PROPERTIES IN THE X*, Y*, Z* COORDINATE SYSTEM FOR THE FULL FOOTPAD MASS DISTRIBUTION ARE

$I^*_{xx} = 292.7 \text{ kg-m}^2$
$I^*_{yy} = 180.5 \text{ kg-m}^2$
$I^*_{zz} = 158.2 \text{ kg-m}^2$
$I^*_{xy} = I^*_{xz} = 0$
$I^*_{yz} = -19.4 \text{ kg-m}^2$

FIGURE 5–8 TRANSFORMATION OF VIKING LANDER INERTIA PROPERTIES

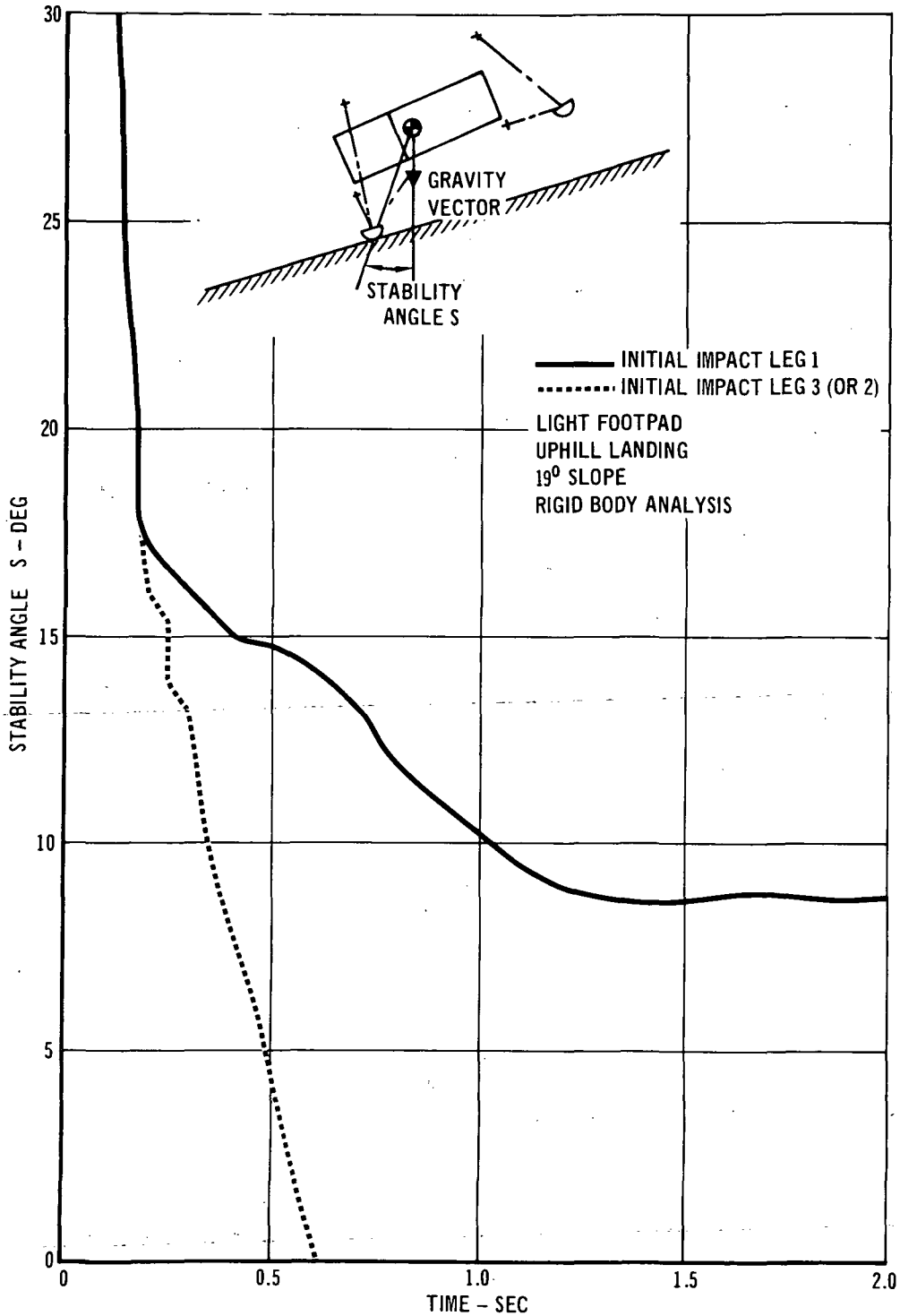

FIGURE 5–9 STABILITY ANGLE COMPARISON FOR DIFFERENCE IN INITIAL FOOTPAD IMPACT

angle in Figures 5-10 through 5-15. The elastic body curves were plotted for the various landing cases employing Mode Set A. In general, the inclusion of structural elasticity had a small effect on lander stability. As illustrated in Figure 5-15, the exception to this is the Downhill Landing for the Light Footpad mass distribution. For a rigid lander, a stable landing resulted at a ground slope angle of 30 degrees, while with structural flexibility (Mode Set A) the lander was not stable above a 24 degree slope.

A comparison between pitch velocities for a rigid lander and an elastic lander is made in Figure 5-16. These curves are for the vehicle with a Light Footpad mass distribution landing downhill on a 30 degree slope and with initial impact occurring on footpad three. Note the higher pitch velocity for the elastic lander following impact of the downhill legs. This indicates that the loads from the downhill legs are causing deformation of the center body structure rather than decreasing the lander's rotational motion. The higher pitch velocity in the elastic body case results in an unstable landing.

In the following paragraphs, comparisons between two cases, one in which elasticity had a large effect on stability and one in which elasticity had negligible effect, are discussed. Both landings were in the downhill direction with the initial impact occurring on footpad three. The Full Footpad mass configuration landed on a 19 degree slope and the Light Footpad mass configuration landed on a 30 degree slope. The elastic body, Full Footpad mass configuration was stable on a 19 degree slope and the elastic body, Light Footpad mass configuration was unstable on a 30 degree slope and as shown in Figure 4-2 was unstable for slopes greater than 24 degrees. In contrast to the elastic body results, the rigid body, Full Footpad mass configuration was stable on a 19 degree slope and the rigid body, Light Footpad mass configuration was stable on a 30 degree slope. See Figures 4-2 and 4-3 for a summary of these results.

As defined in Reference 1, the elastic body generalized coordinates define the time varying response of the center body modes used to represent structural elasticity. Time histories of the elastic body generalized coordinates for the four lowest frequency modes of Mode Set A and the above mentioned 19 degree slope case are presented in Figure 5-17. The same parameters for the 30 degree slope condition are shown in Figure 5-18. The generalized coordinate for the highest frequency mode is not shown since there was negligible response of this mode for both cases.

As noted in Figures 5-17 and 5-18, the response of all the modes, except elastic mode 5, 15.88 Hz, are similar. For the unstable 30 degree slope case, the response in this 15.88 Hz mode is quite high following impact of the downhill legs. The large response in this mode accounts for the large effect of structural elasticity on stability for the 30 degree slope case.

For these two landing conditions, 30 and 19 degree slopes, the difference in response of the 15.88 Hz mode is related to the impact time phasing of the downhill legs, legs one and two. The timing of the main strut loads for the downhill legs, and the response of the 15.88 Hz mode for these two landing conditions, are shown in Figure 5-19. The main strut loads are compared since

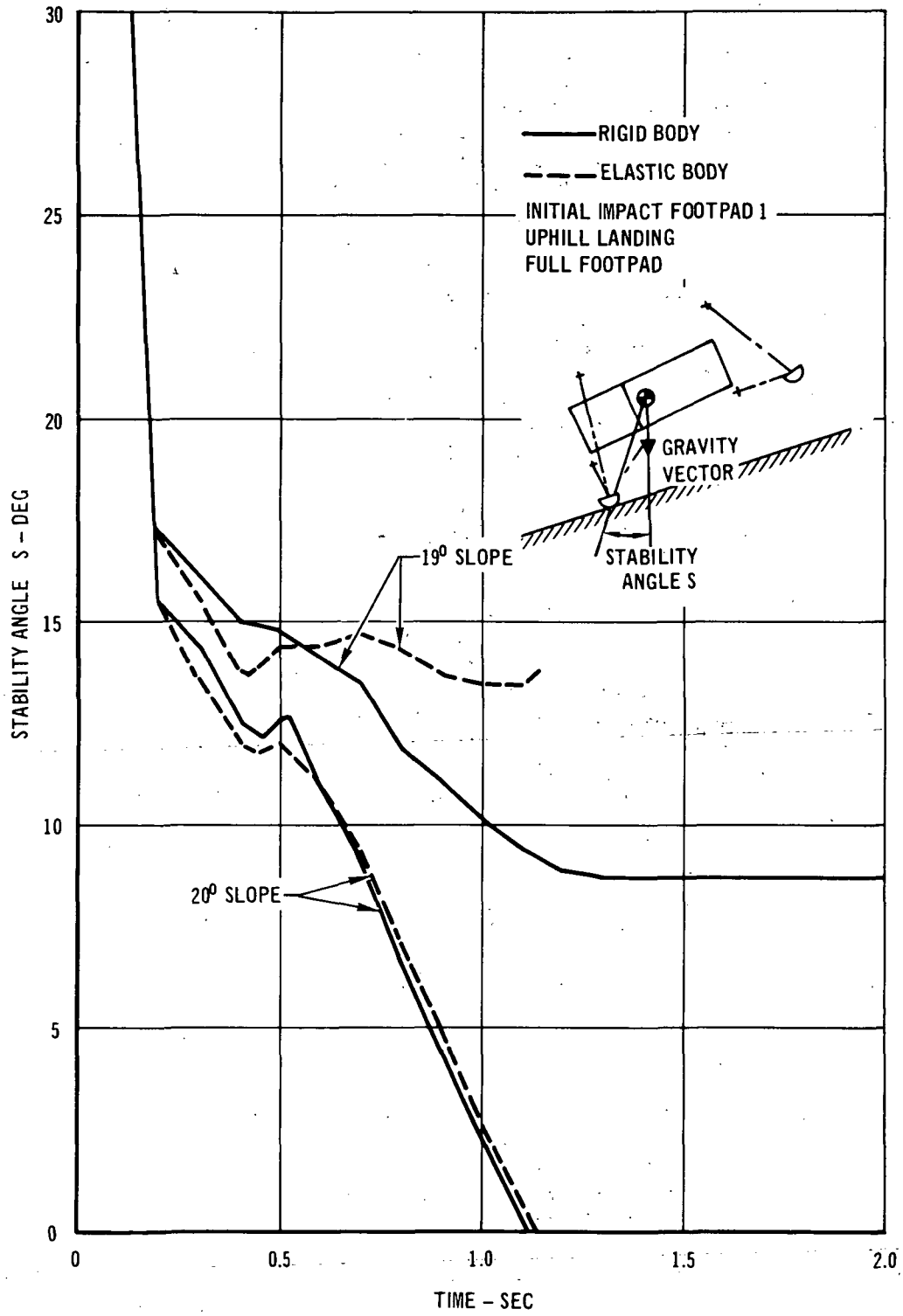

FIGURE 5–10 RIGID AND ELASTIC BODY STABILITY ANGLE COMPARISON FOR UPHILL LANDING AND INITIAL IMPACT OF FOOTPAD ONE

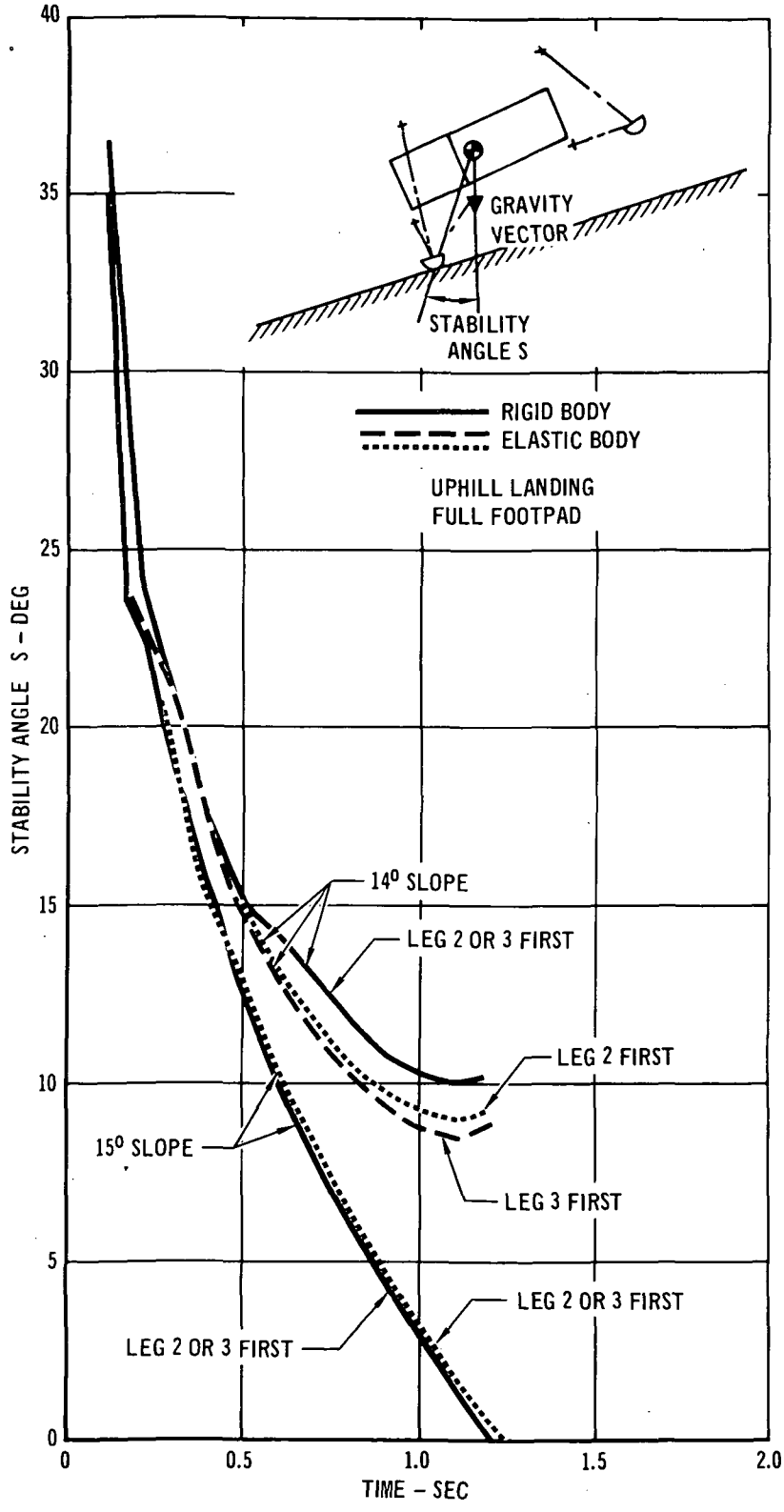

FIGURE 5-11 RIGID AND ELASTIC BODY STABILITY ANGLE COMPARISON FOR UPHILL LANDING AND INITIAL IMPACT OF FOOTPAD TWO OR THREE

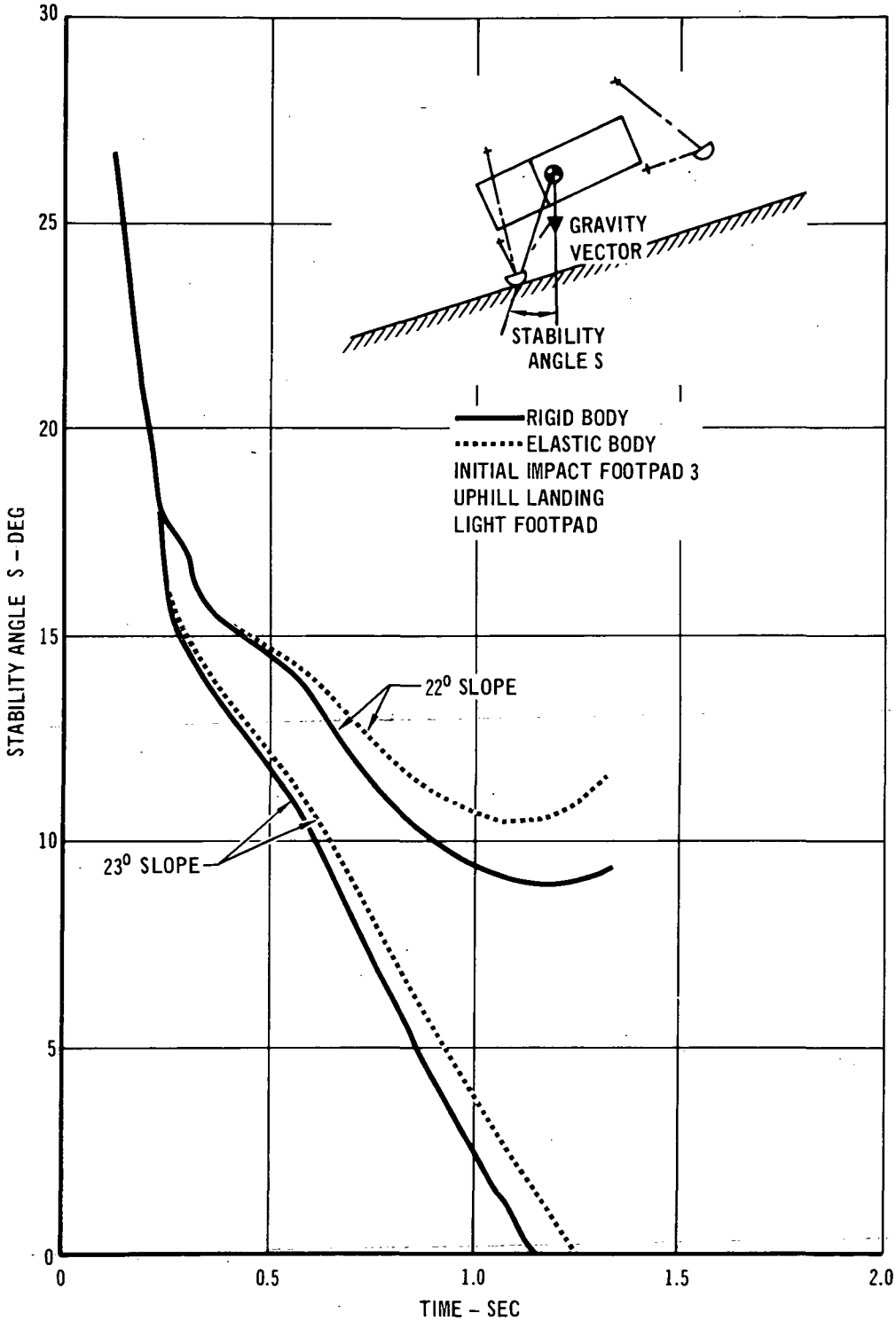

FIGURE 5–12 RIGID AND ELASTIC BODY STABILITY ANGLE COMPARISON FOR UPHILL LANDING AND LIGHT FOOTPAD MASS DISTRIBUTION

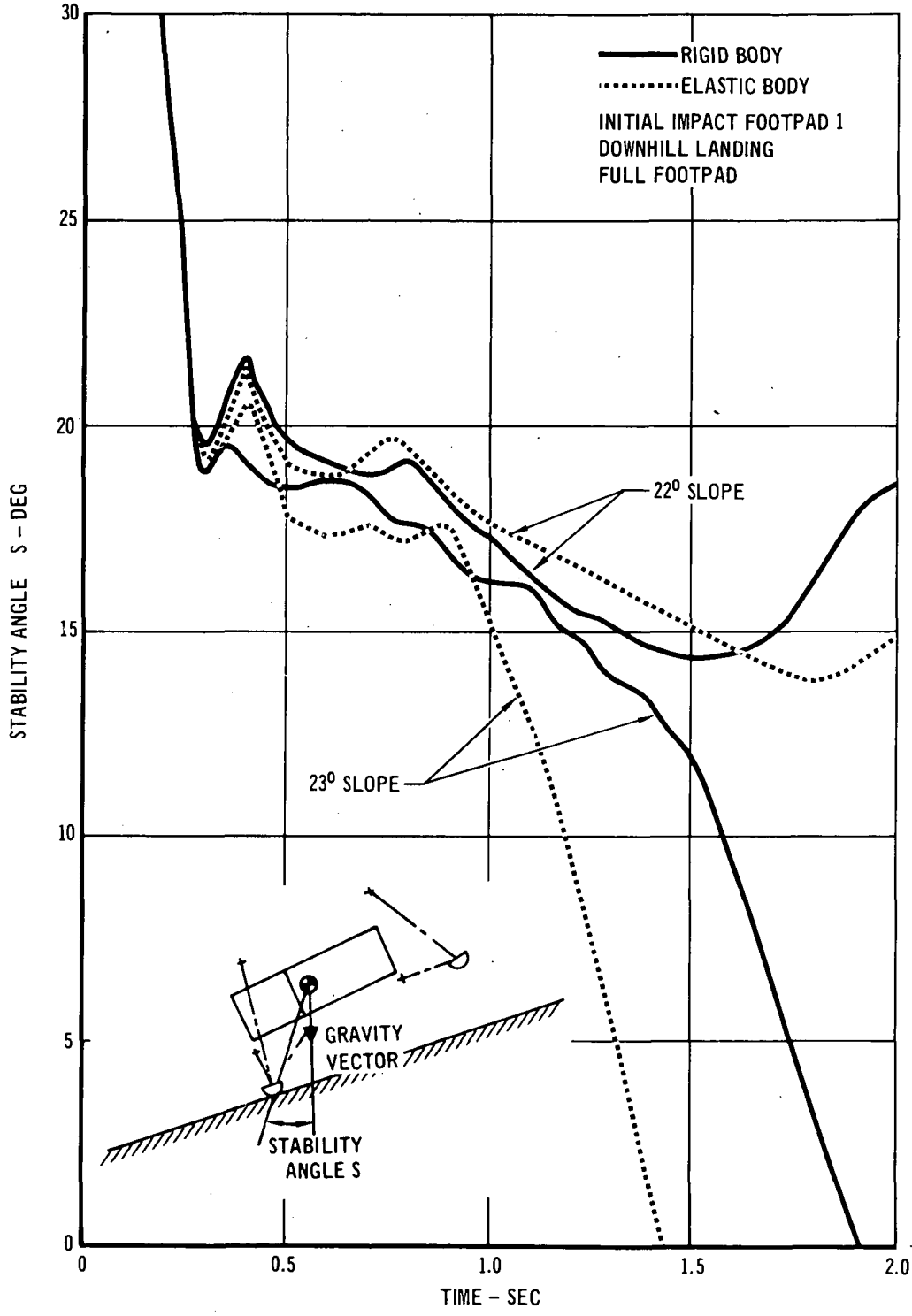

FIGURE 5–13 RIGID AND ELASTIC BODY STABILITY ANGLE COMPARISON FOR DOWNHILL LANDING AND INITIAL IMPACT OF FOOTPAD ONE

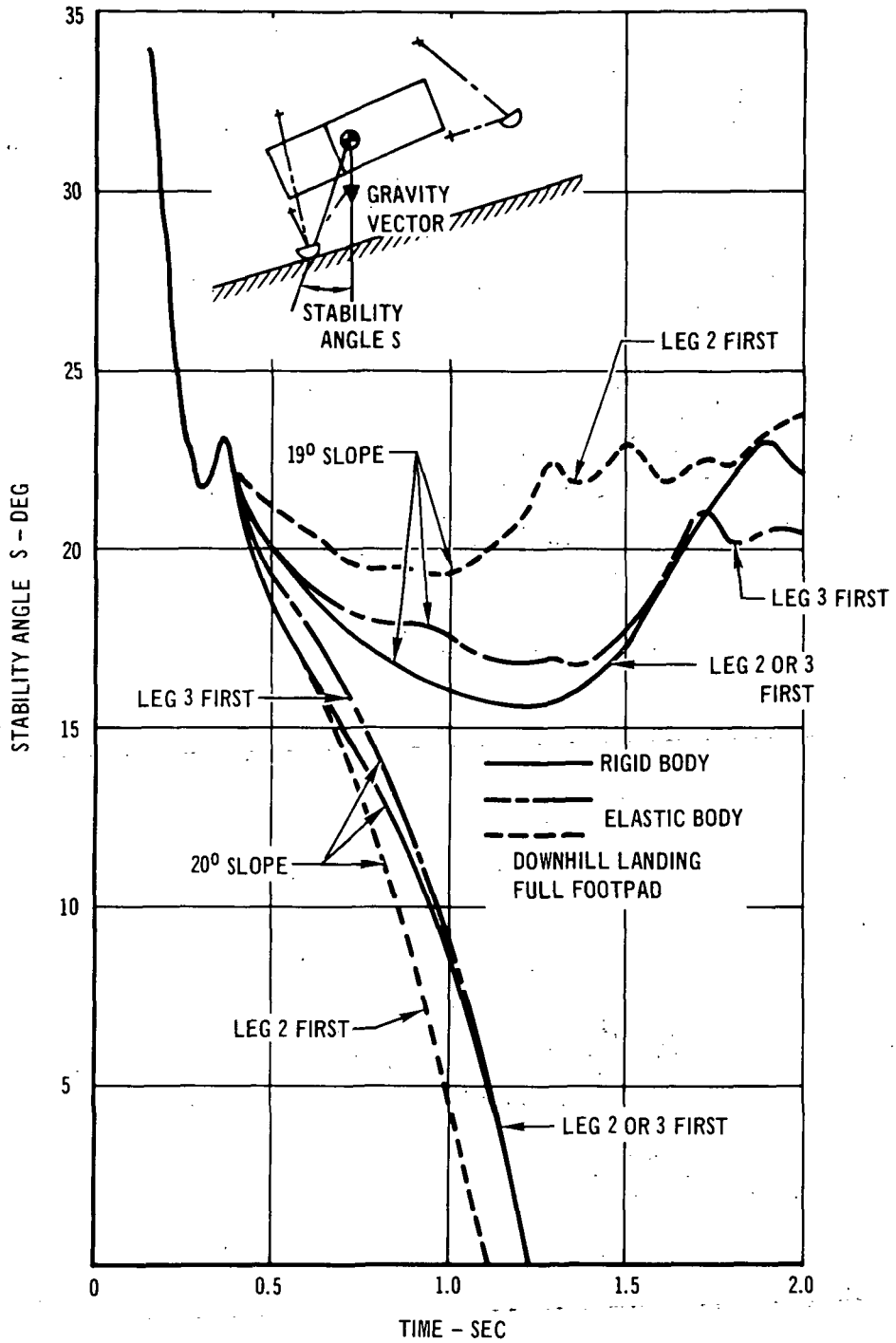

FIGURE 5-14 RIGID AND ELASTIC BODY STABILITY ANGLE COMPARISON FOR DOWNHILL LANDING AND INITIAL IMPACT OF FOOTPAD TWO OR THREE

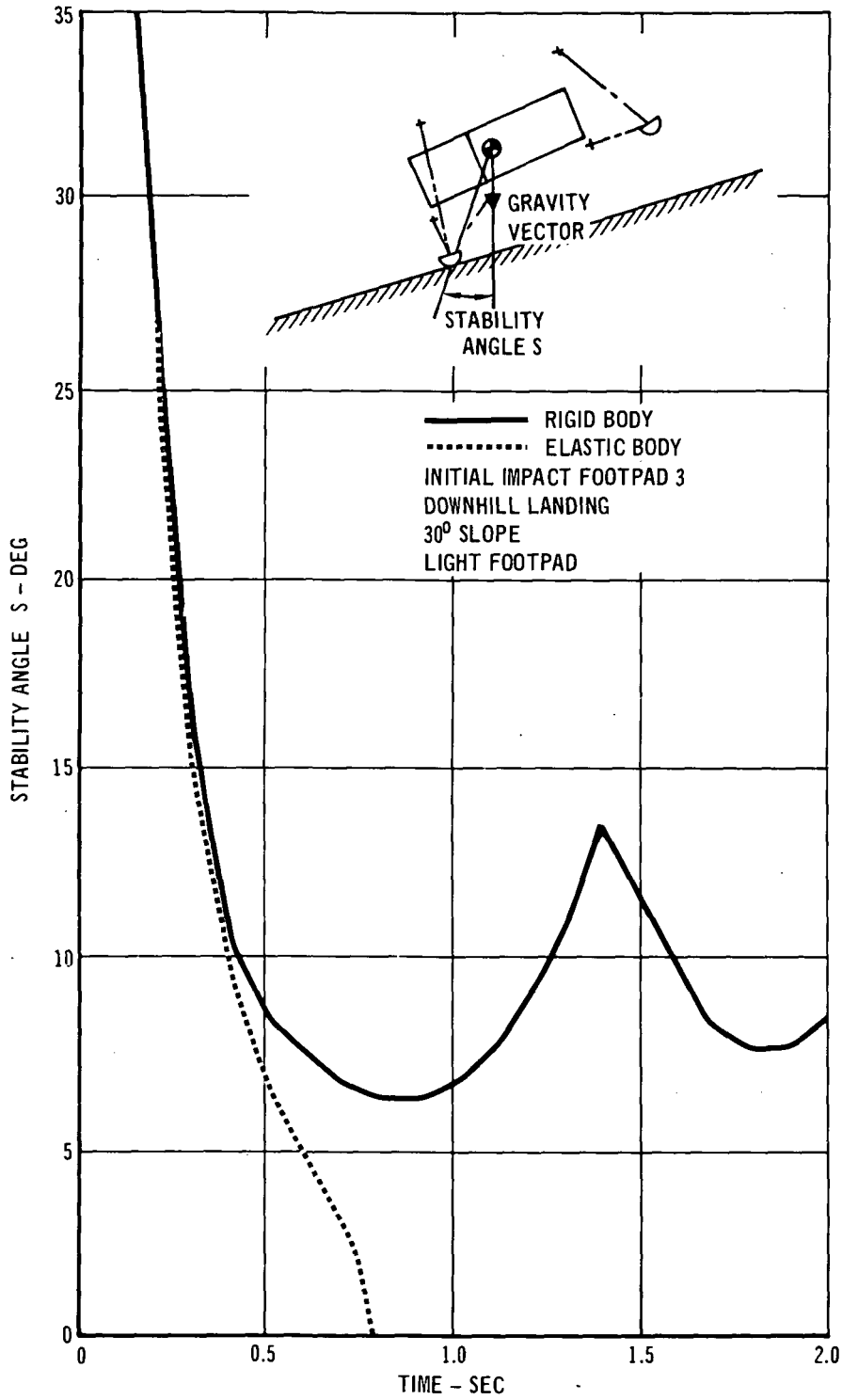

FIGURE 5–15 RIGID AND ELASTIC BODY STABILITY ANGLE COMPARISON FOR DOWNHILL LANDING AND LIGHT FOOTPAD MASS DISTRIBUTIONS

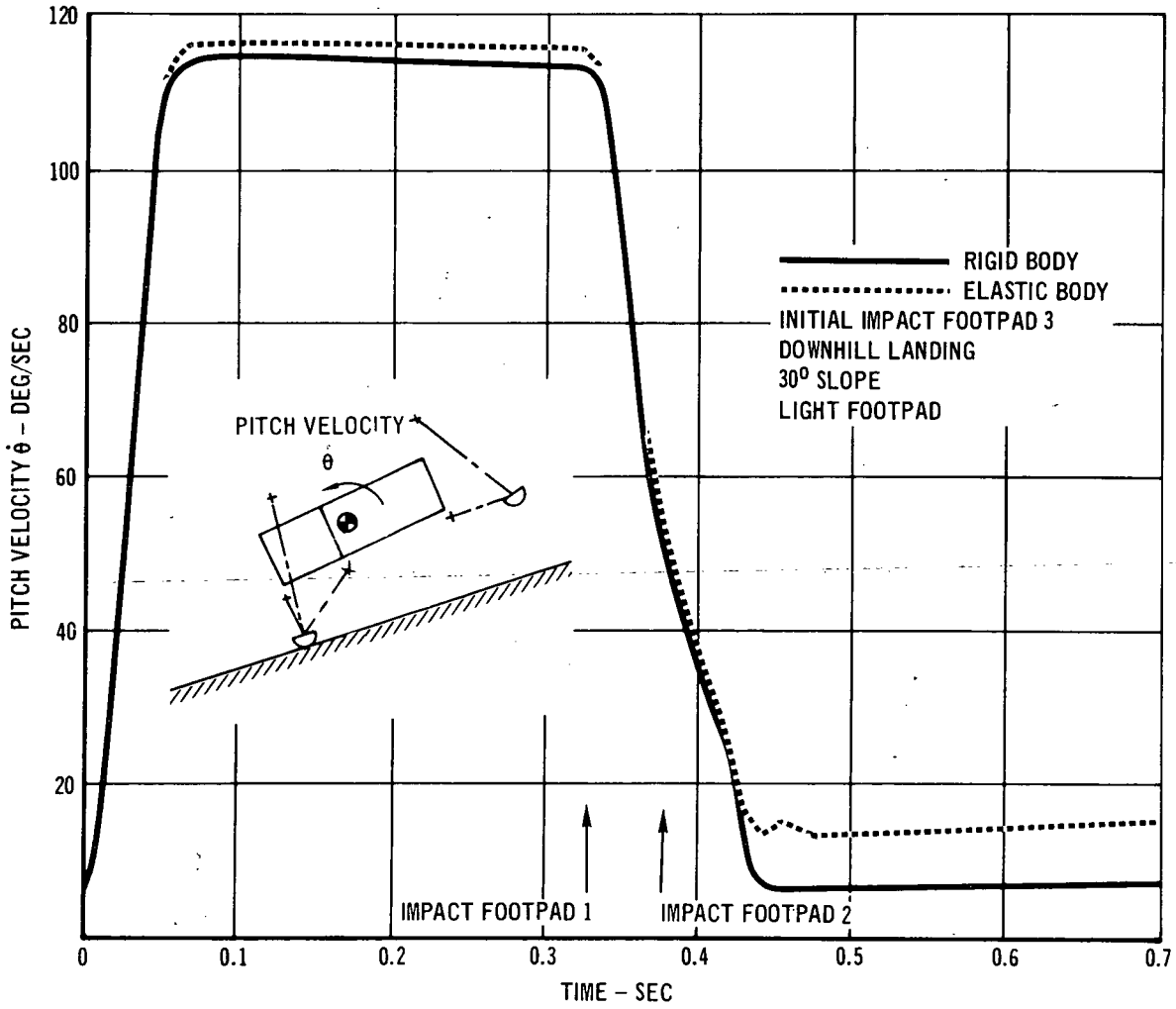

FIGURE 5–16 COMPARISON OF PITCH VELOCITY FOR RIGID AND ELASTIC BODY ANALYSIS

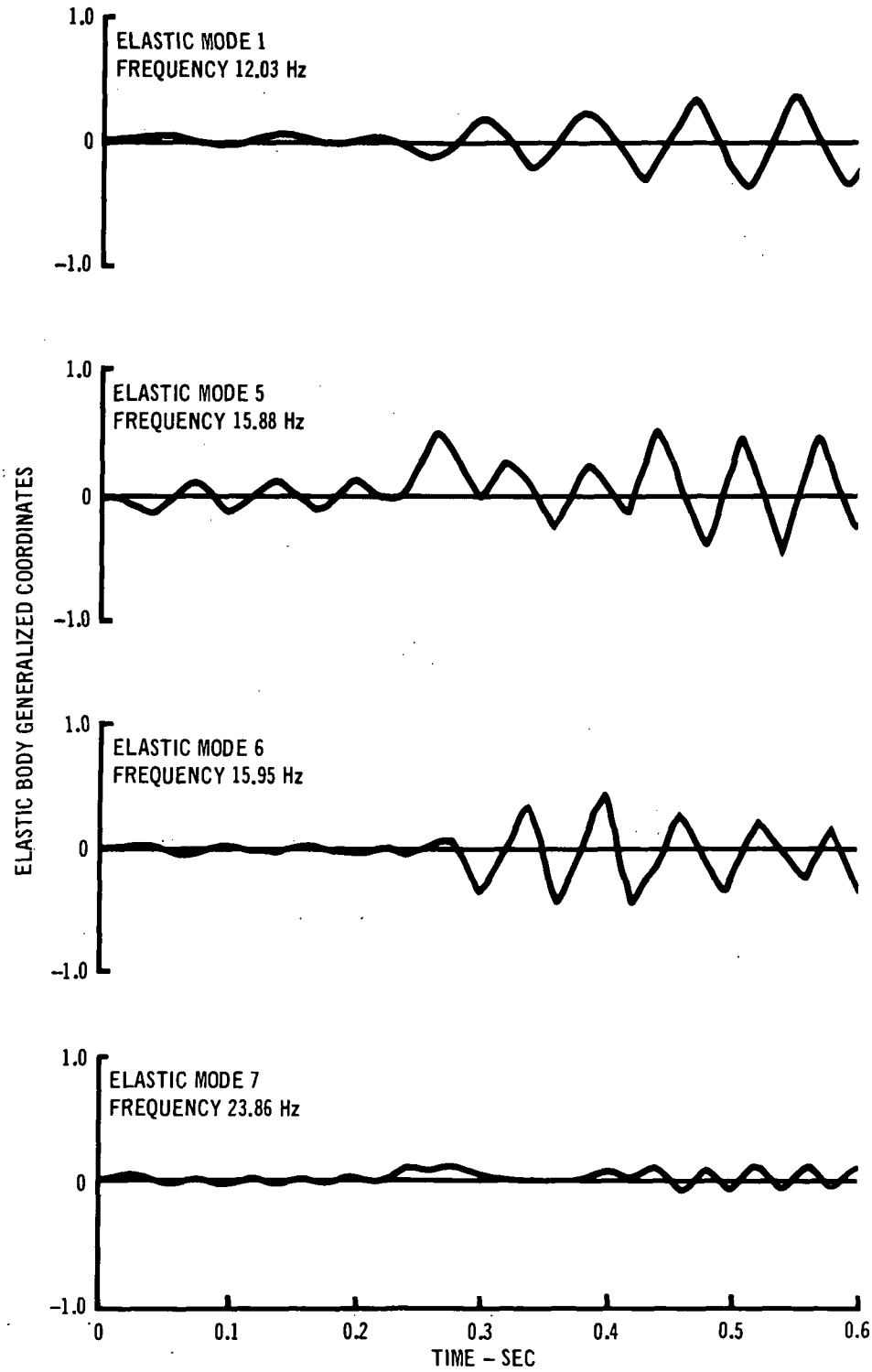

FIGURE 5-17 ELASTIC BODY GENERALIZED COORDINATES FOR FULL FOOTPAD DOWNHILL LANDING ON A 19 DEGREE SLOPE

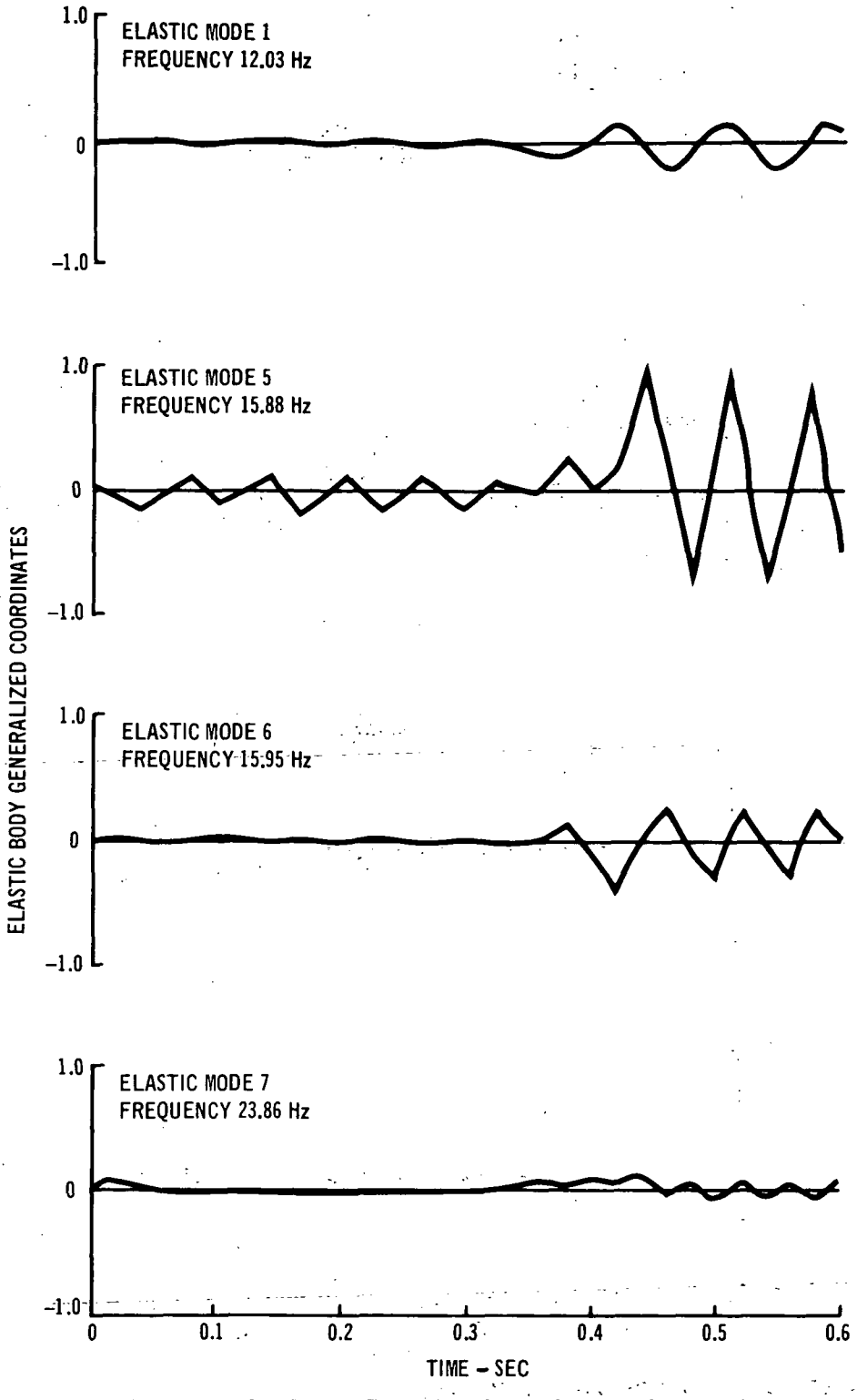

FIGURE 5–18 ELASTIC BODY GENERALIZED COORDINATES FOR LIGHT FOOTPAD DOWNHILL LANDING ON A 30 DEGREE SLOPE

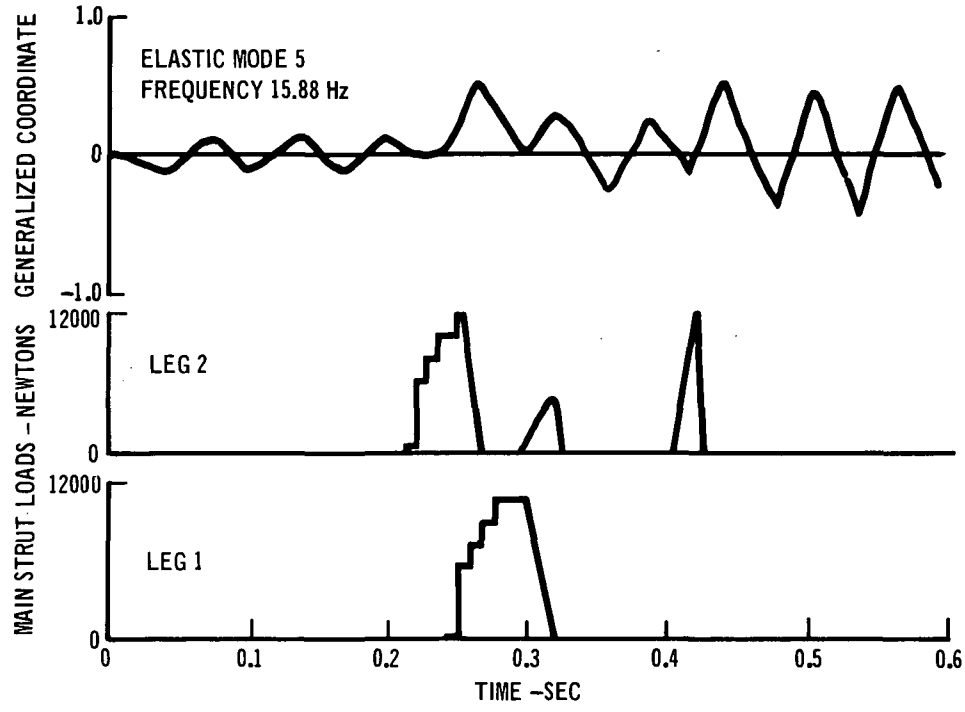

(A) Downhill Landing, Full Footpad, 19° Slope

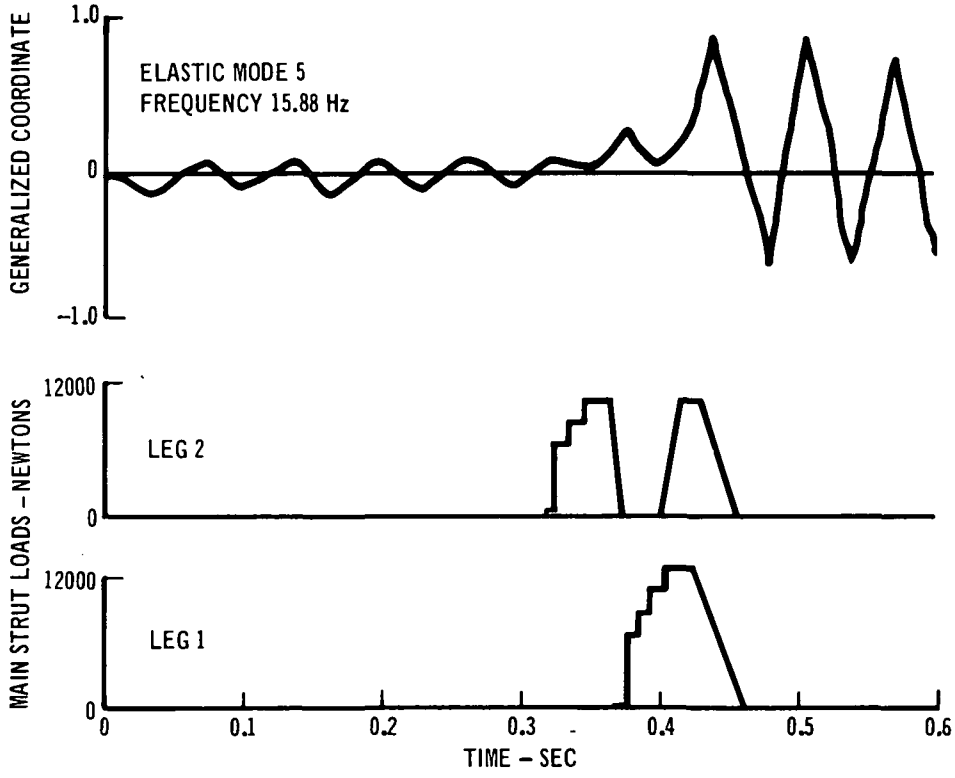

(B) Downhill Landing, Light Footpad, 30° Slope

FIGURE 5–19 FOOTPAD IMPACT TIMING EFFECTS ON RESPONSE OF 15.88 H_z MODE

these are the most important in exciting this mode (see Figure A-3). In the 19 degree slope case, Figure 5-19A, the leg two main strut load tends to counteract the residual elastic motion in the 15.88 Hz mode resulting from the initial leg three impact. The following leg one main strut load again excites this mode to the amplitude indicated in Figure 5-19A near a time of 0.26 seconds.

The effect of these strut loads on the 15.88 Hz mode is quite different for the 30 degree slope case, Figure 5-19B. Again the leg two main strut load tends to suppress the residual elastic motion. However, the timing of the leg one main strut load and a second pulse of the leg two main strut load is such that a high response in the 15.88 Hz mode results near a time of 0.44 seconds. This results in the large response of this mode and consequent significant effect of structural elasticity on landing stability for the 30 degree slope case.

6.0 CONCLUSIONS

Analytical landing studies have been conducted to assess the effects of structural elasticity on stability of the Viking Lander. In addition, the effects on landing stability of the nonsymmetric nature of both the lander inertia properties and center body mode shapes have been evaluated. Two landing conditions and two assumed lander mass and inertia distributions were considered during these investigations.

The following conclusions may be made from these study results:

1. Lander flexibility can have a large effect on landing stability as illustrated for the Light Footpad mass distribution and a Downhill Landing. In this case, a six degree difference resulted between the ground slope for a stable landing with rigid body and elastic body lander representations. However, for the remaining cases run during Task Order Six, the inclusion of structural flexibility had negligible effect on the stability of the Viking Lander.

2. Nonsymmetric inertia properties of the Viking Lander have a large effect on landing stability. For the same landing condition and assumed lander mass and inertia distribution, depending on which footpad made initial ground impact, as much as a five degree difference in critical ground slope angle resulted.

3. Assumed lander mass and inertia distributions are important in assessing Viking Lander stability. When a majority of the footpad mass (and inertia effects) was included with the center body mass and inertia properties, the predicted critical ground slopes were higher than when the total footpad mass was associated with the footpad motion.

The effects of lander inertia properties, footpad/center body mass distribution, and structural elasticity on landing stability of the Viking Lander are discussed (Section 5.0) in terms of the particular lander configuration and two specific landing conditions considered during Task Order Six. Additional effort would be required to fully evaluate the effects of these parameters on landing stability. Therefore, care must be exercised in drawing conclusions concerning the overall stability characteristics of the Viking Lander from these results.

This Page Intentionally Left Blank.

7.0 REFERENCES

1. Otto, O. R.; Laurenson, R. M.; Melliere, R. A., and Moore, R. L.: "Analyses and Limited Evaluation of Payload and Legged Landing System Structures for the Survivable Soft Landing of Instrument Payloads," NASA CR-111919, July 1971.

2. Letter 126/NAS1-8137-6, National Aeronautics and Space Administration, Langley Research Center, Hampton, Virginia, 23365, 13 December 1971.

3. Data Transmittal Letter, Martin Marietta Corporation, Denver Division, Denver, Colorado 80201, 9 February 1972.

4. Greenwood, Donald T., Principles of Dynamics, Prentice-Hall, Inc., Englewood Cliffs, New Jersey, 1965, pp 297-302.

5. Enclosure 2, Letter 466-E231-041, McDonnell Douglas Astronautics Company - East, St. Louis, Missouri, 63166, 16 May 1972.

This Page Intentionally Left Blank.

APPENDIX A

VIKING LANDER MODAL DATA

Free-free modes for the Viking Lander were provided by Martin Marietta Corporation, Reference 3. The first 35 elastic modes were reviewed and four sets of five modes each were selected for the consideration of structural elasticity effects during the Task Order Six stability studies. These 35 modes covered a frequency range up to approximately 75 Hz. This frequency range was felt to be sufficient to assess the effects of elasticity on landing stability. The criteria in establishing the mode sets and a summary of these sets is contained in Section 3.2.

A summary of the 35 Viking Lander modes reviewed is given in Figure A-1. Indicated in this figure is the location on the lander of predominant modal deformation for each mode. Also, the modes contained in each mode set, Figure 3-9, are noted in Figure A-1.

Plots of the mode shapes for the modes included in the four mode sets are given in Figures A-2 through A-16. On these plots Main 1, etc., refers to the main strut attach points and Load Limit 1A, etc., refers to the load alleviator/drag strut attach points.

ELASTIC MODE	FREQUENCY Hz	LOCATION OF PREDOMINANT MOTION	MODE SET
1	12.03	MAIN STRUT 3	A
2	12.35	TANKS 1 & 2	
3	12.47	TANKS 1 & 2	
4	14.21	MET HEAD	
5	15.88	MAIN STRUTS 1 & 2	A & D
6	15.95	MAIN STRUTS 1 & 2	A
7	23.86	CAMERA 2	A & D
8	31.90	CAMERA 2	
9	34.32	SB HGA MAST	
10	35.24	ENGINE 2	
11	36.20	SB HGA MAST	
12	36.96	CAMERA 1	
13	37.45	CAMERA 1	
14	38.30	CAMERAS 1 & 2	
15	39.29	MET HEAD	
16	40.21	MET HEAD	
17	40.44	ENGINE 2	
18	41.74	SOIL BOOM	A
19	43.57	ENGINE 2	
20	43.77	ENGINE 2	
21	45.43	CAMERA 2	B
22	45.99	MAIN STRUT 3	B
23	47.11	ALL MAIN STRUTS	B & D
24	50.21	MAIN STRUT 1	B & D
25	51.86	MAIN STRUT 2	B
26	53.07	TANK 2	C & D
27	54.86	TANK 1	C
28	56.24	DAPU	C
29	60.61	MAIN STRUT 1	C
30	61.17	CAMERA 1	
31	67.95	SOIL BOOM	C
32	69.14	SB HGA MECH	
33	71.50	SOIL BOOM	
34	73.84	CAMERA 1	
35	75.36	LOAD LIMITER 2B	

FIGURE A–1 SUMMARY OF VIKING LANDER MODAL DATA

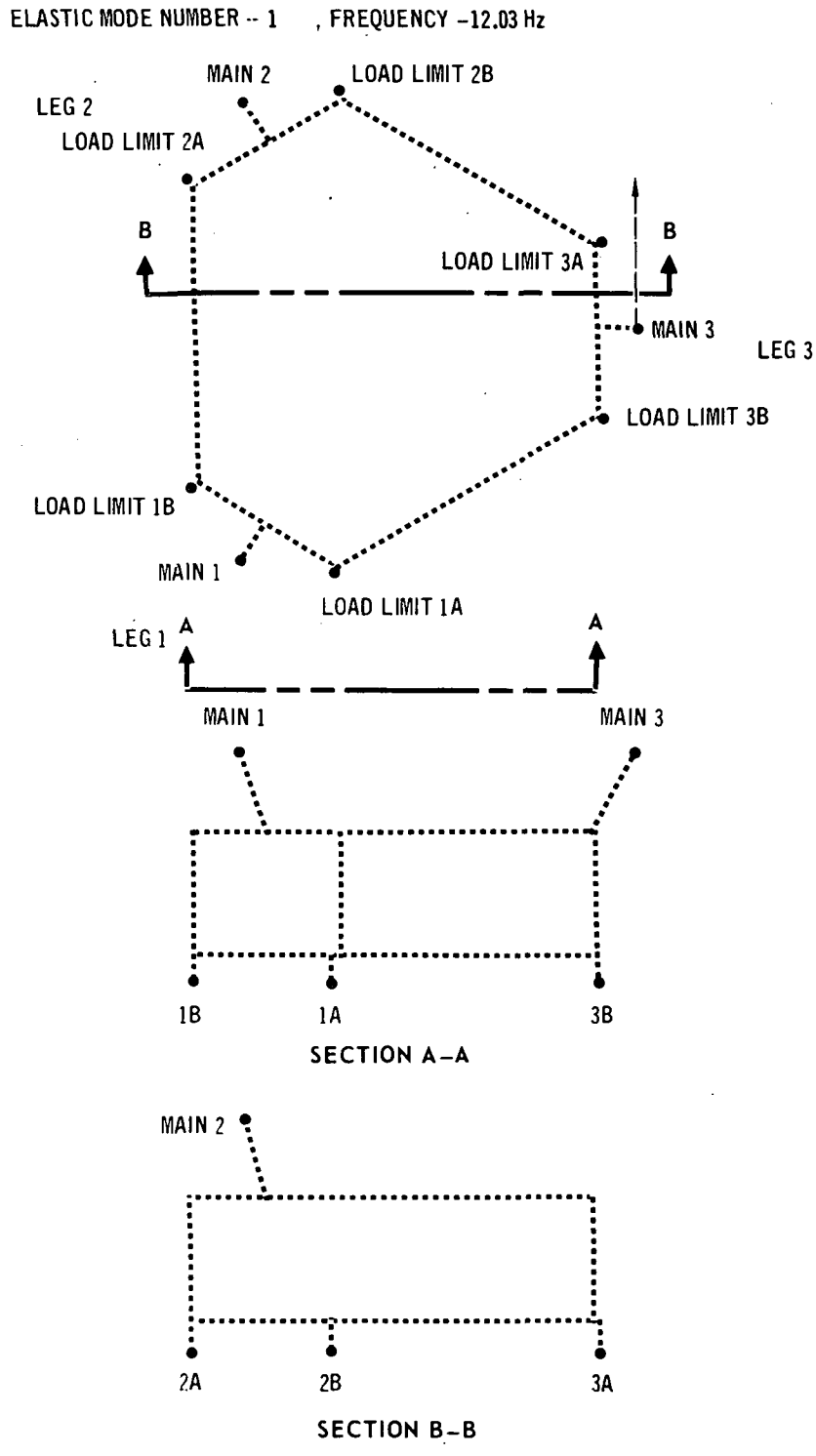

FIGURE A–2 VIKING LANDER MODE SHAPE

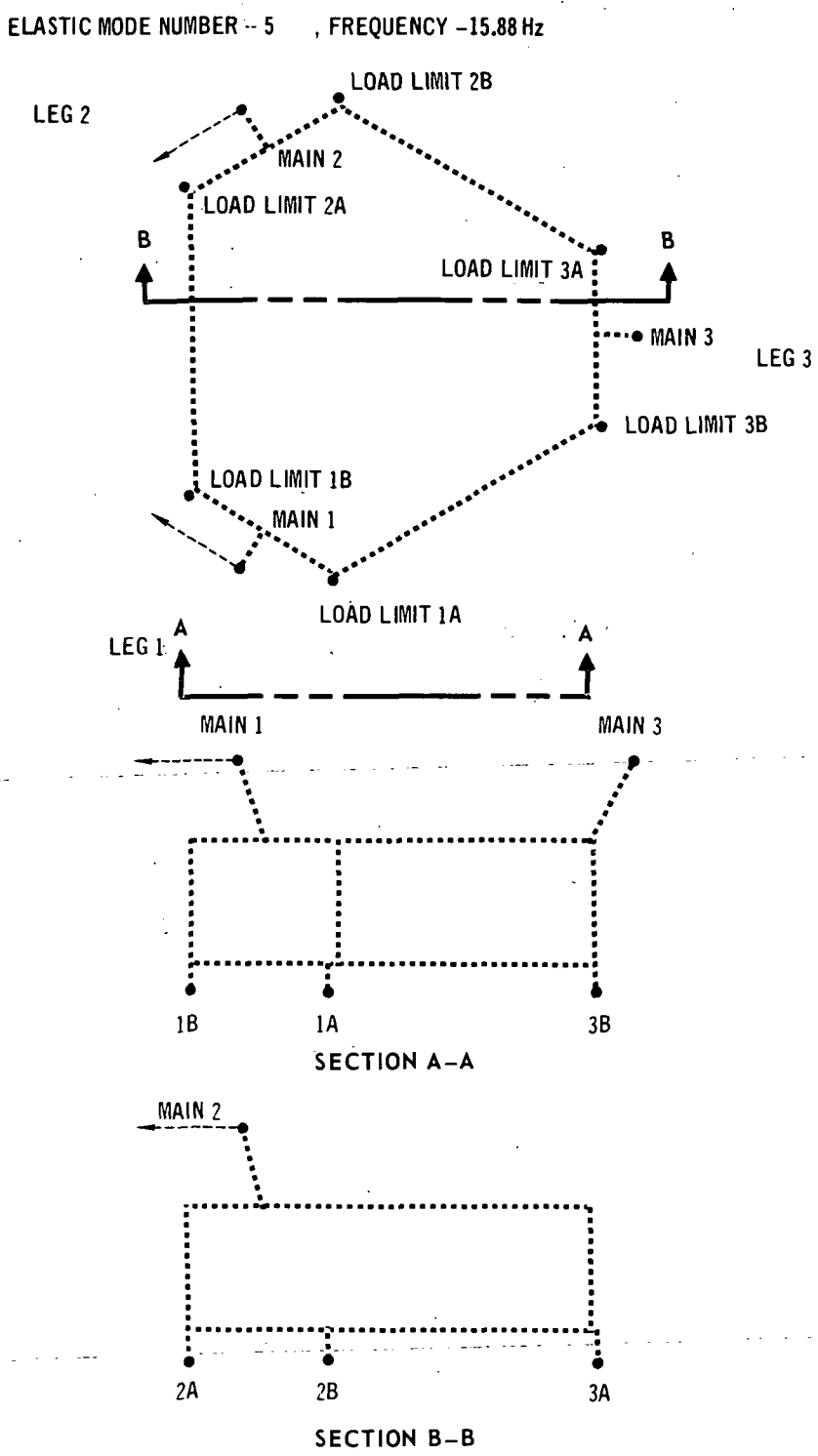

FIGURE A–3 VIKING LANDER MODE SHAPE

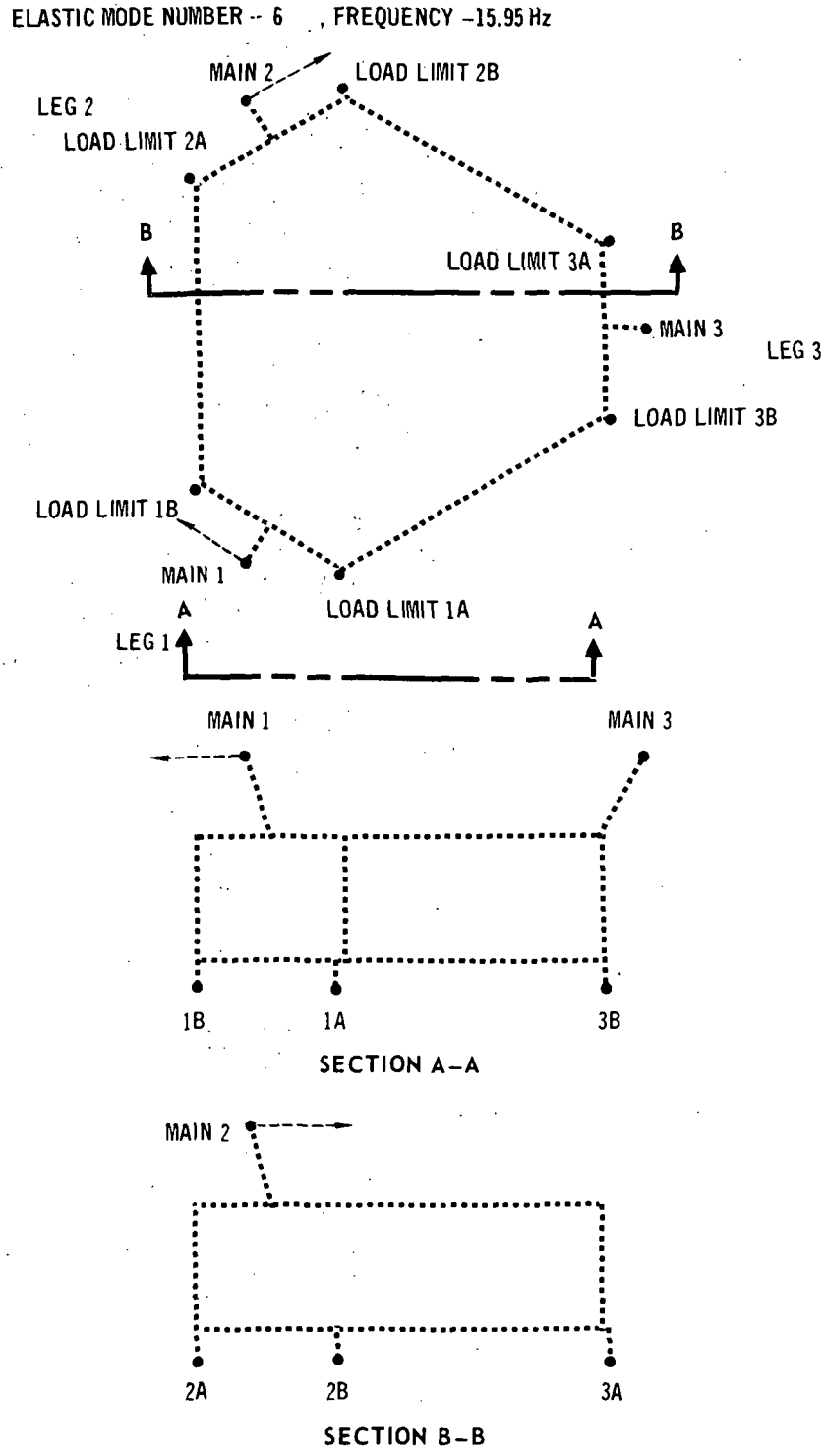

FIGURE A-4 VIKING LANDER MODE SHAPE

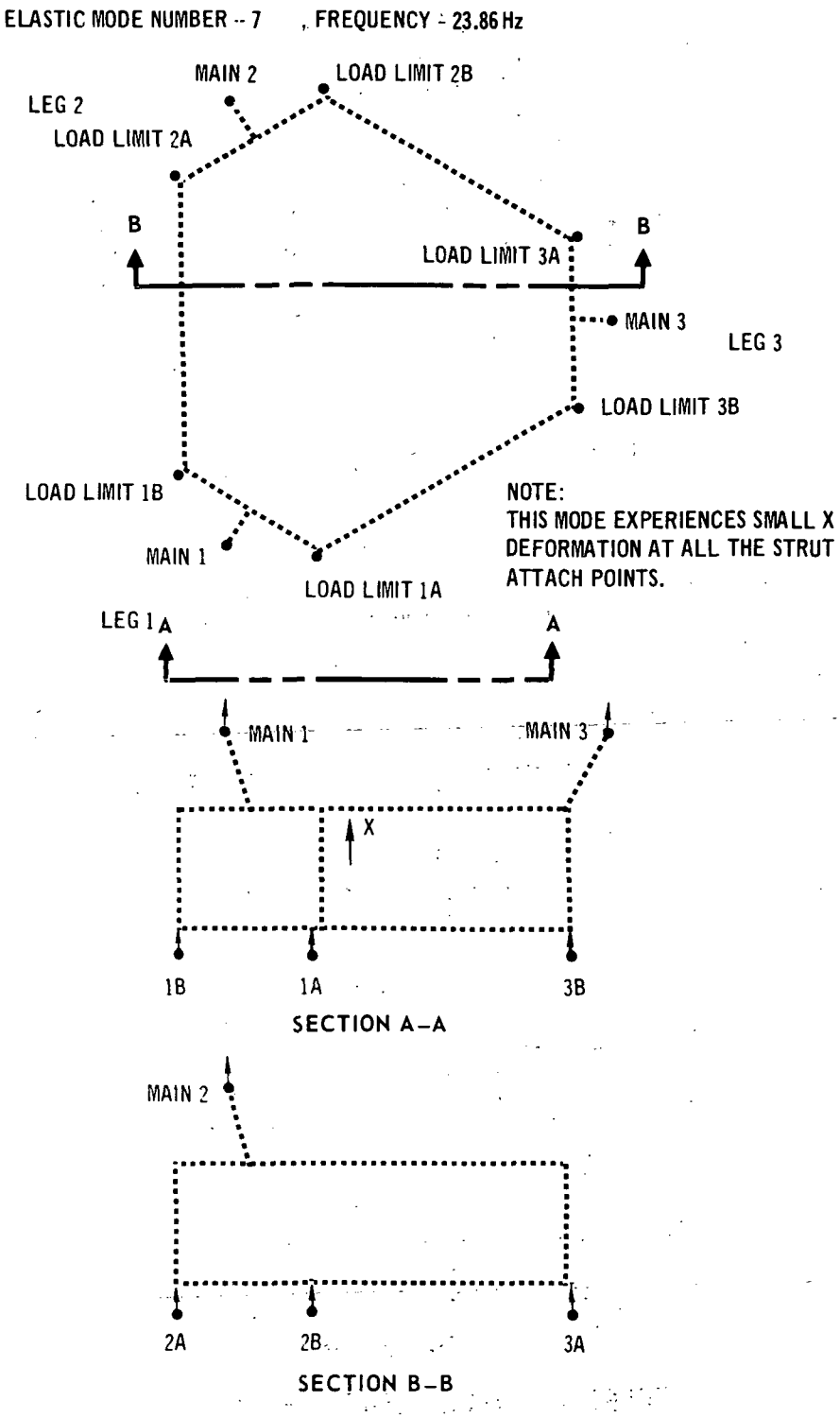

FIGURE A–5 VIKING LANDER MODE SHAPE

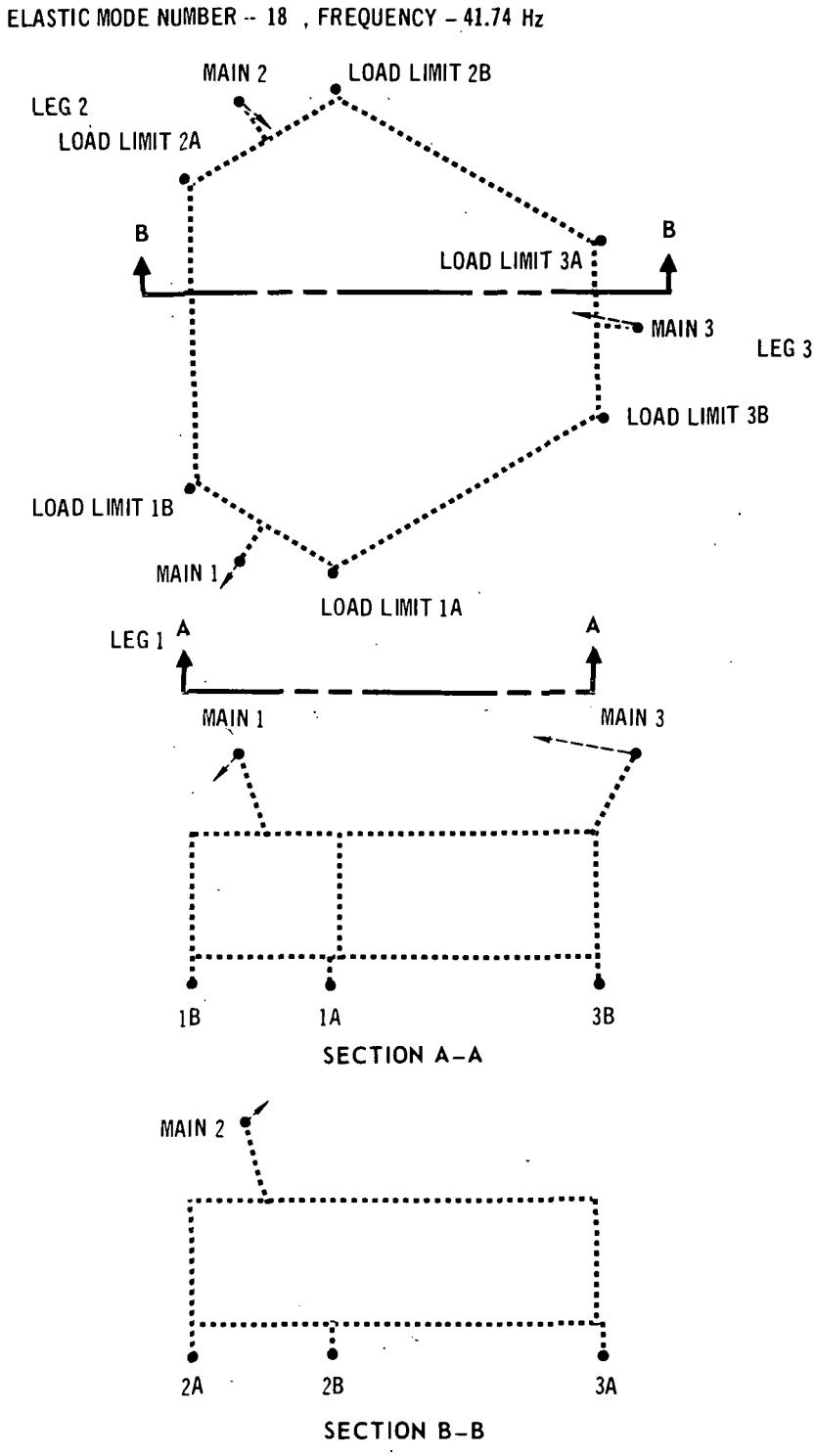

FIGURE A-6 VIKING LANDER MODE SHAPE

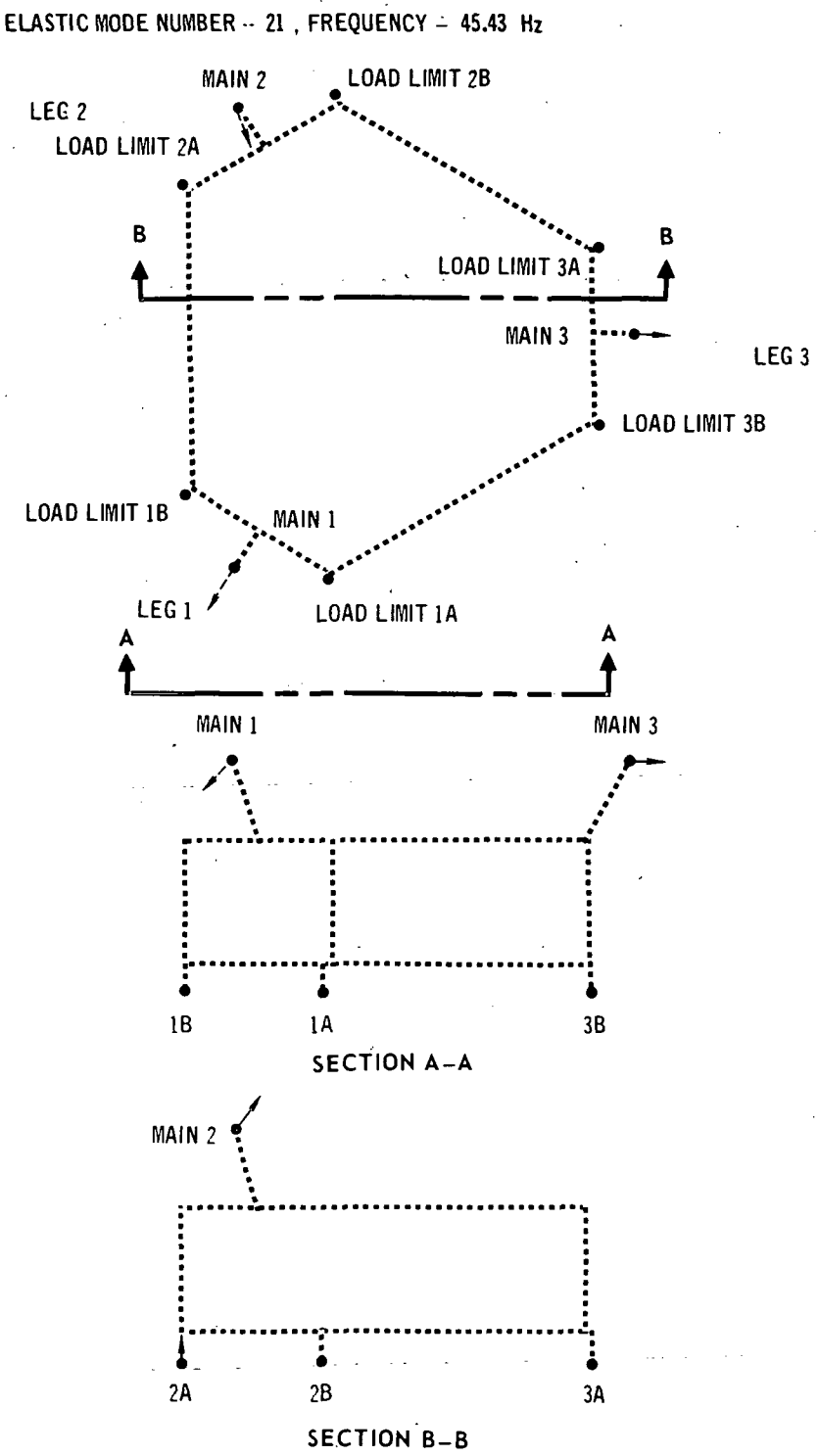

FIGURE A–7 VIKING LANDER MODE SHAPE

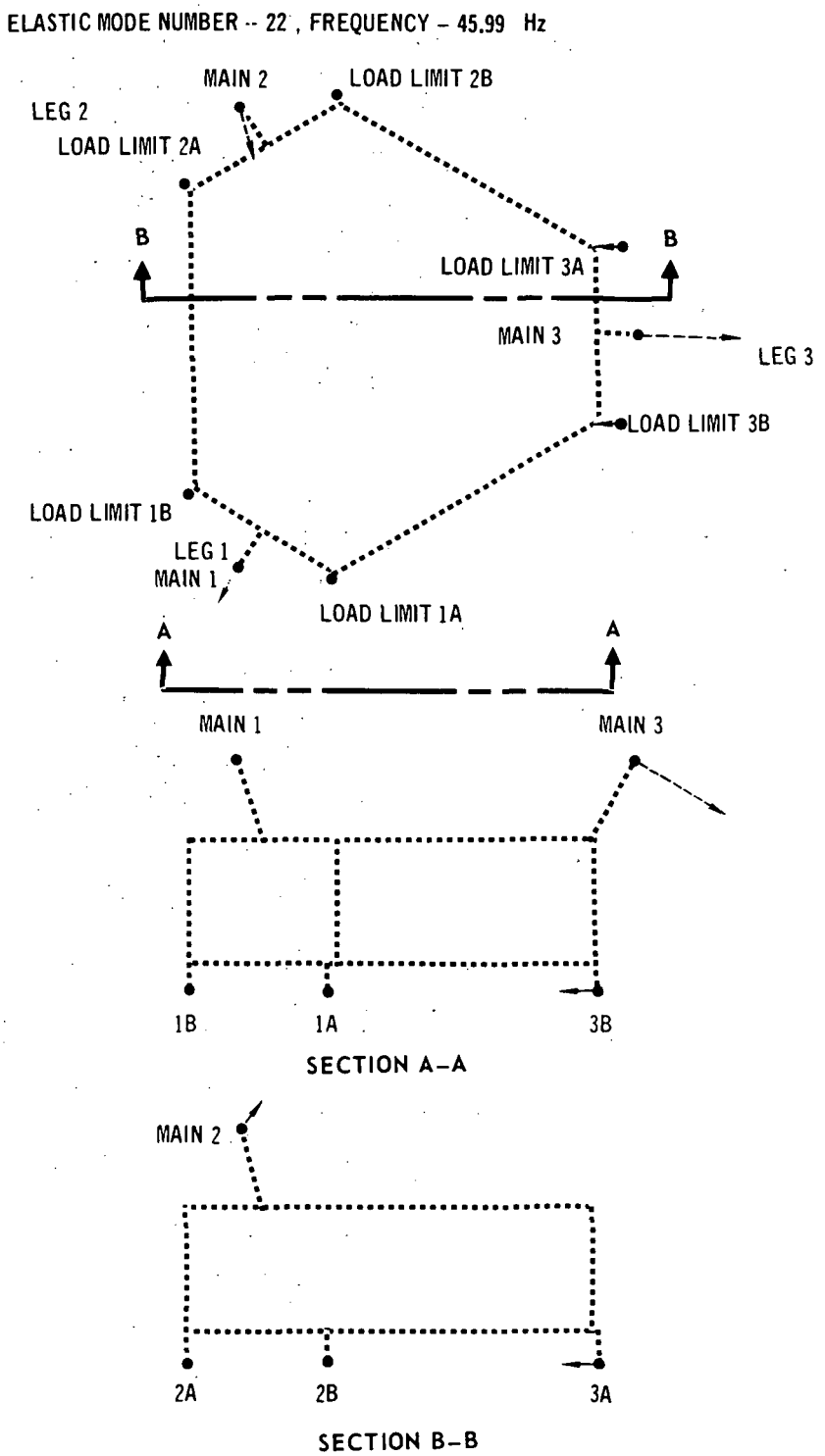

FIGURE A-8 VIKING LANDER MODE SHAPE

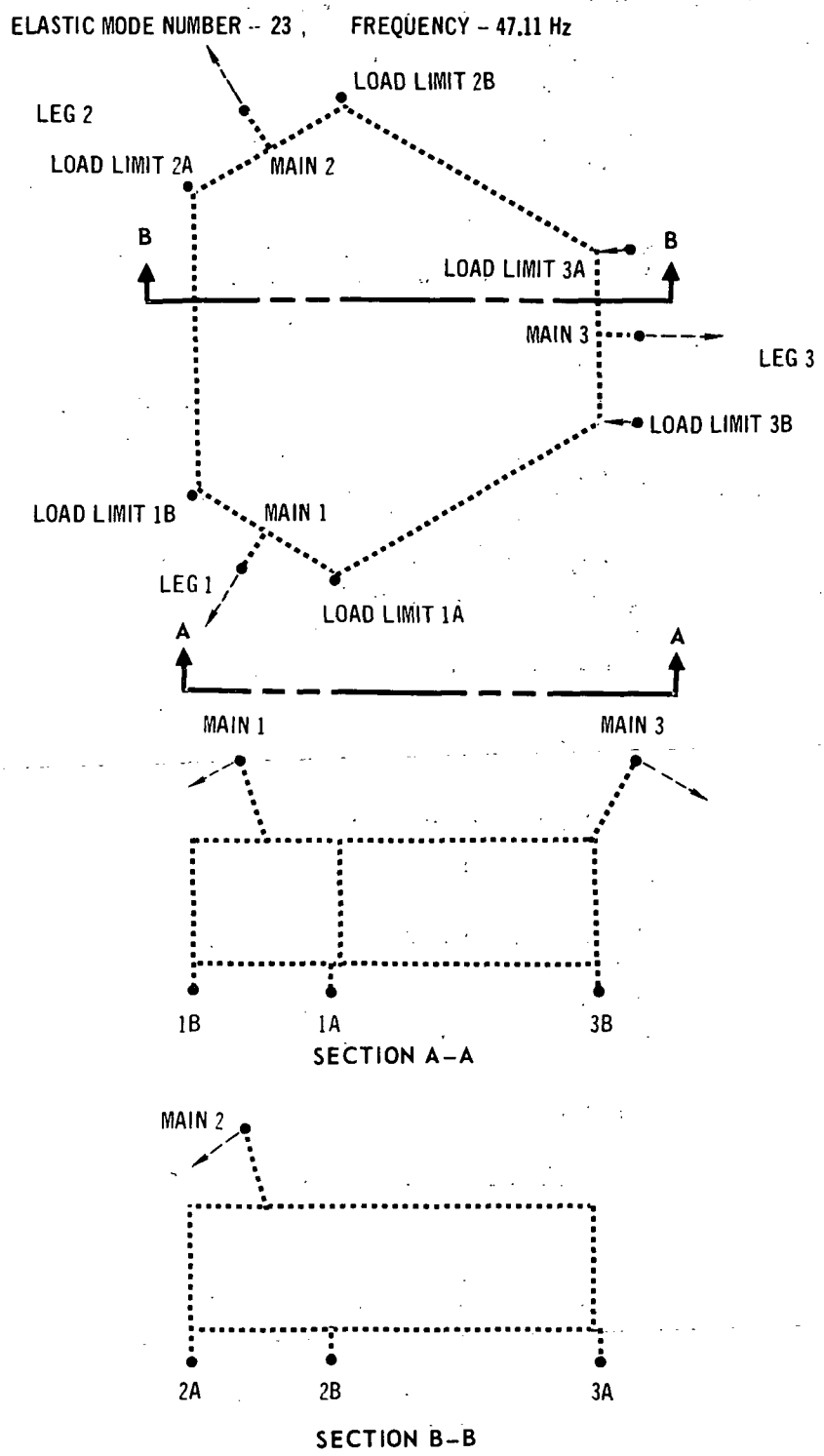

FIGURE A–9 VIKING LANDER MODE SHAPE

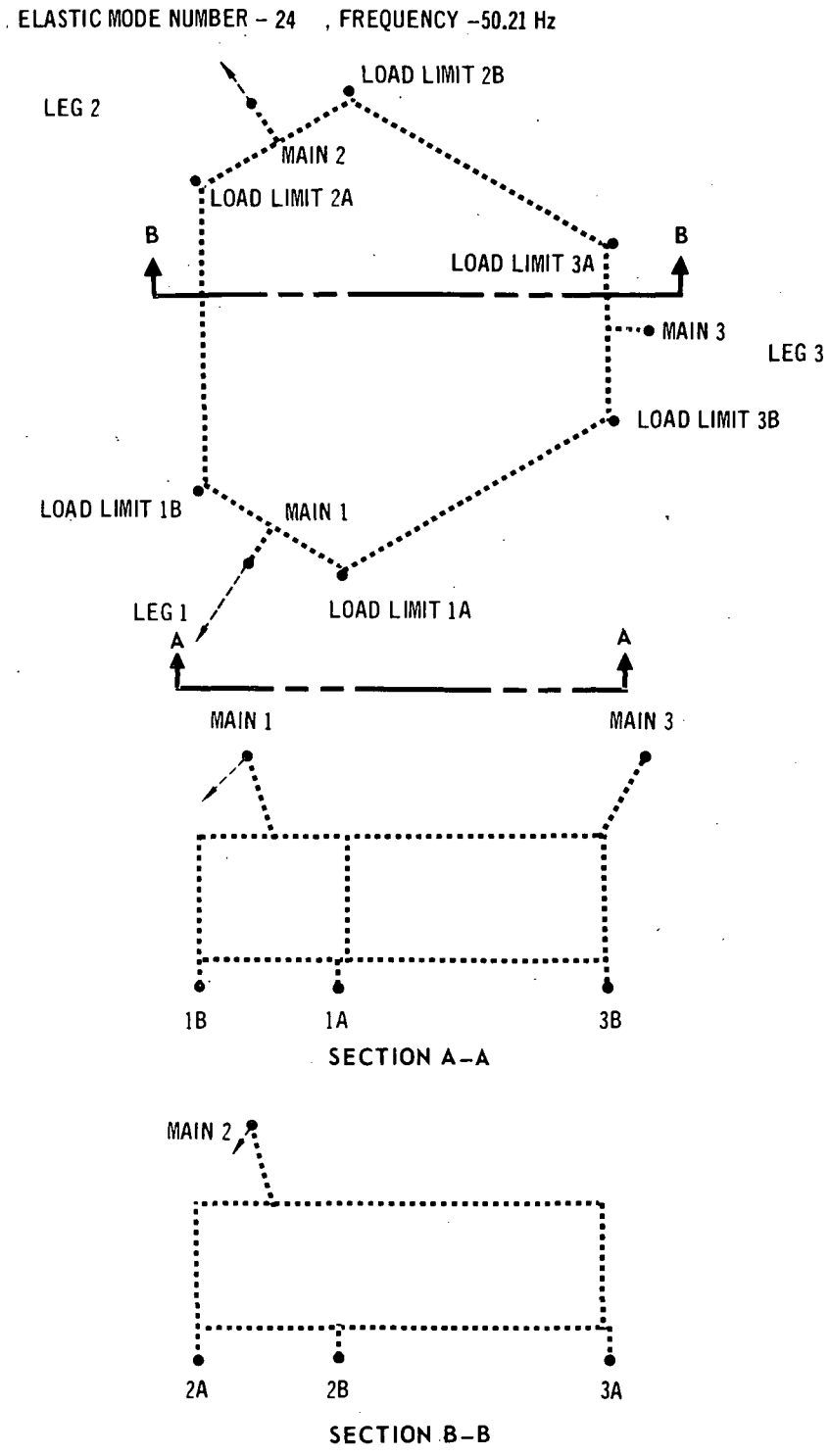

FIGURE A–10 VIKING LANDER MODE SHAPE

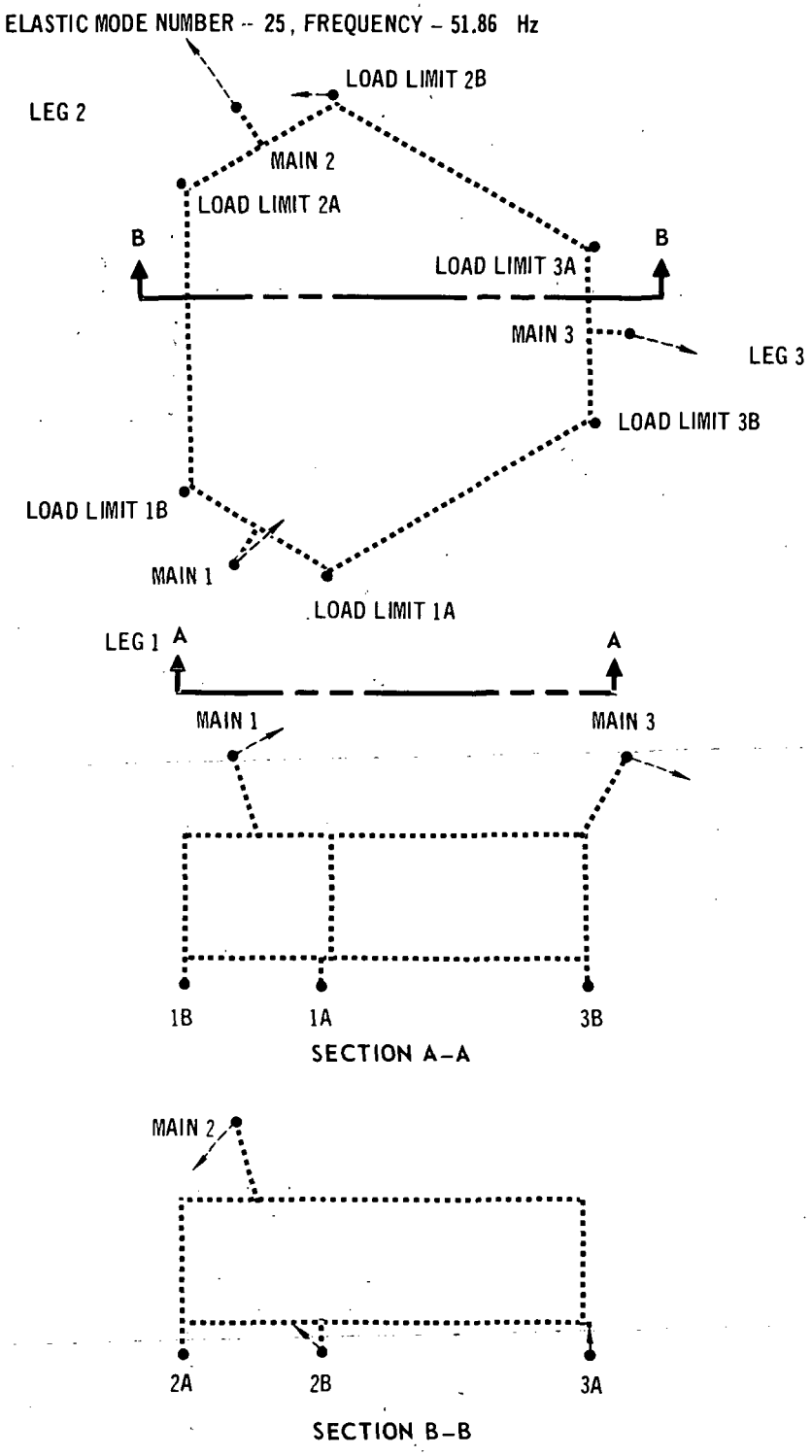

FIGURE A-11 VIKING LANDER MODE SHAPE

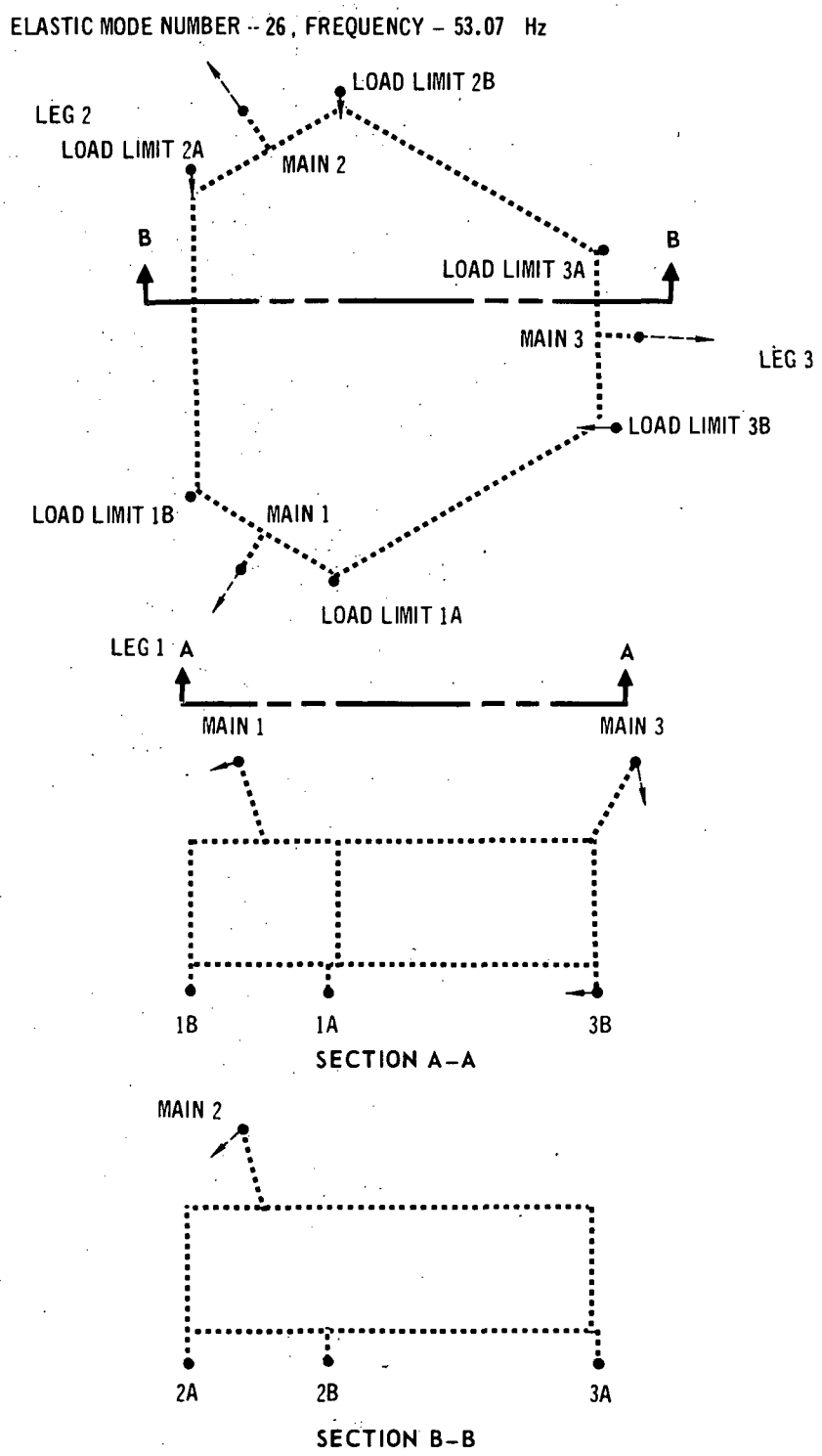

FIGURE A–12 VIKING LANDER MODE SHAPE

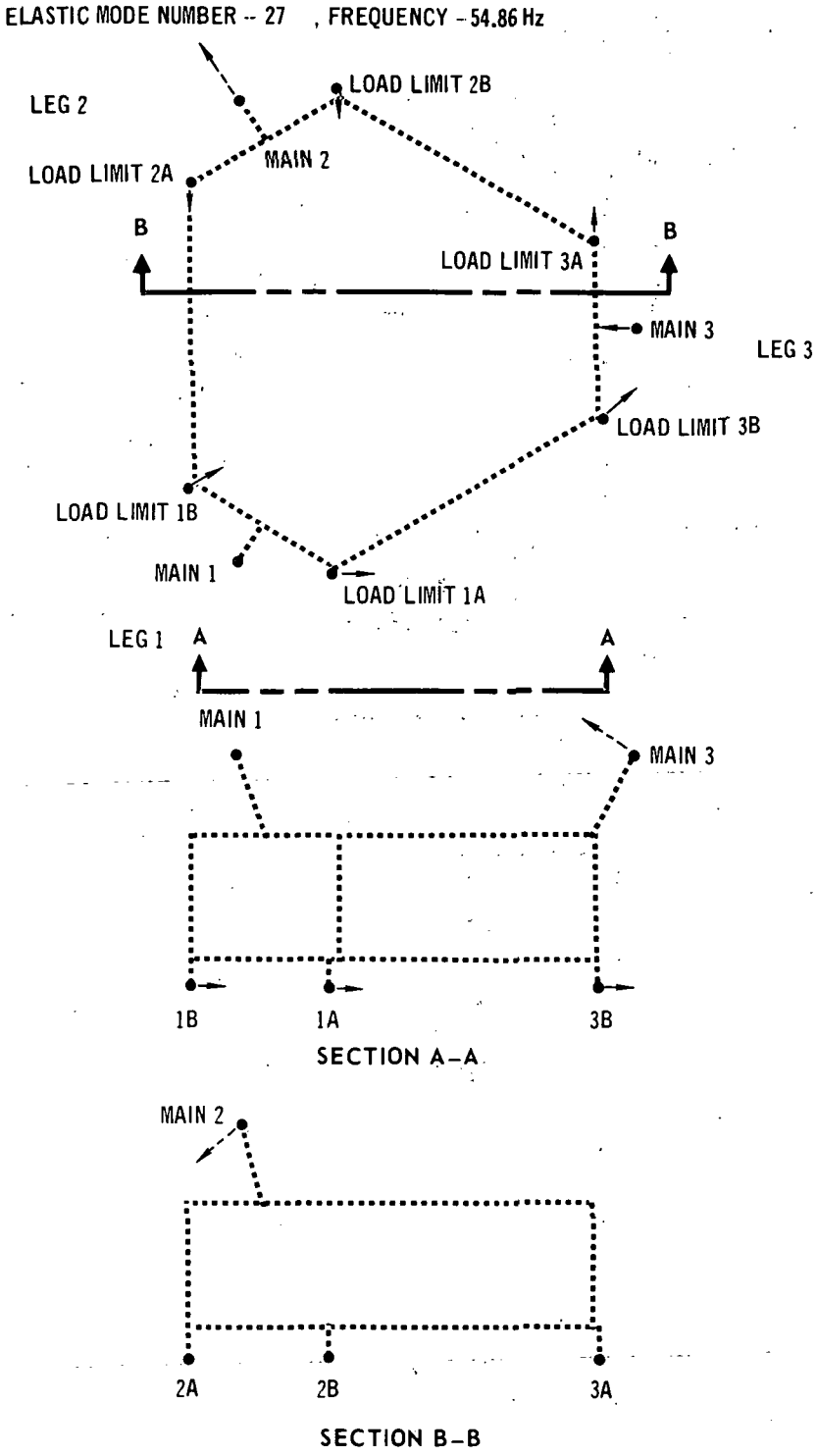

FIGURE A–13 VIKING LANDER MODE SHAPE

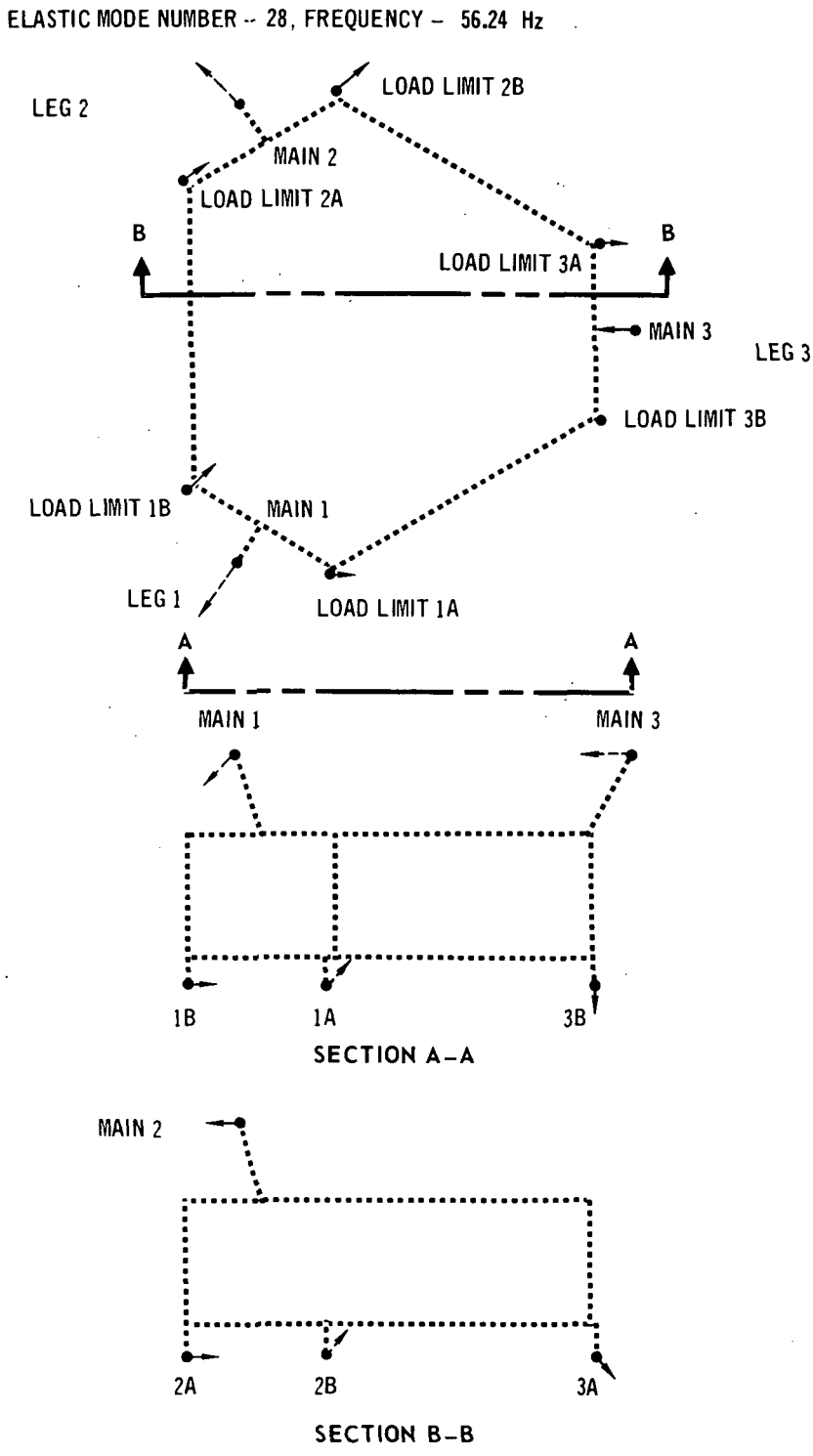

FIGURE A–14 VIKING LANDER MODE SHAPE

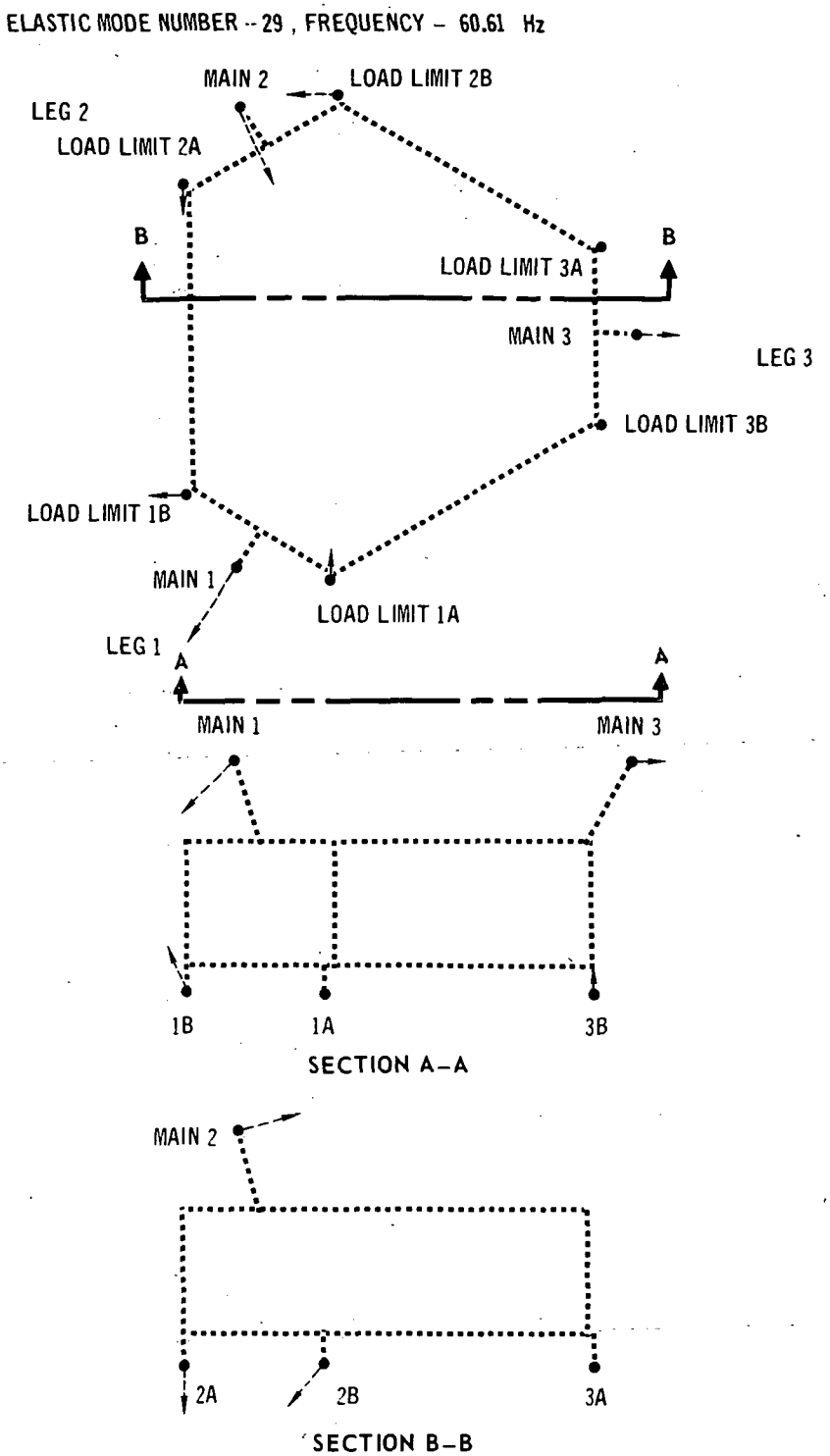

FIGURE A–15 VIKING LANDER MODE SHAPE

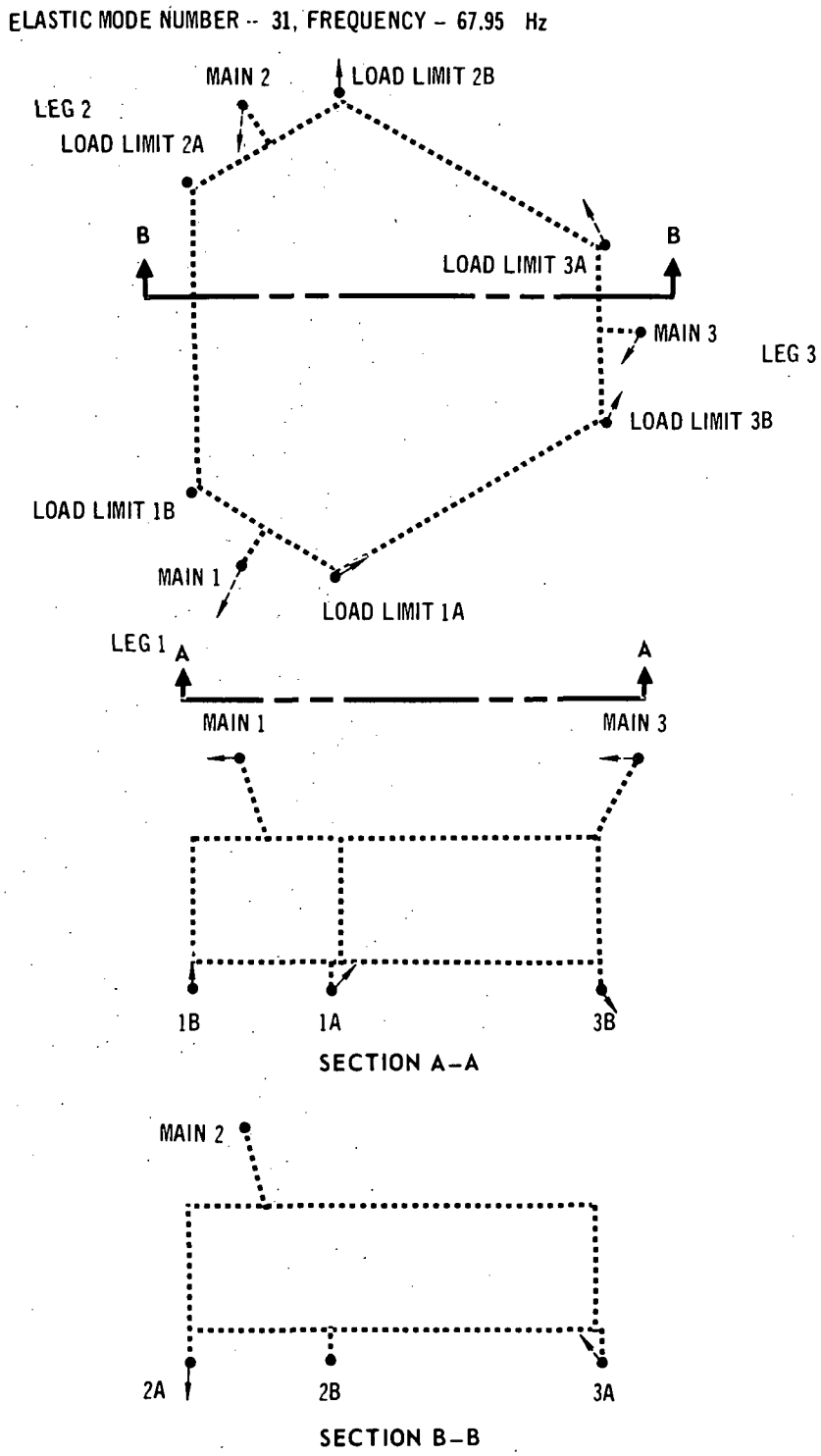

FIGURE A-16 VIKING LANDER MODE SHAPE

APPENDIX B

DETAILS OF VIKING LANDER DRAG STRUT AND LOAD ALLEVIATOR IDEALIZATION

Modifications in subroutine STRUT of the Landing Loads and Motions Program, Reference 1, were made during Task Order Six to allow idealization of the load stroke characteristics of the Viking Lander drag strut and load alleviator combination. This idealization and the landing program input data requirements are detailed in Reference 5.

As discussed in Section 3.1, the effective drag strut load stroke curve was the series combination of the load alleviator and drag strut load stroke characteristics. A typical effective drag strut load stroke curve is shown in Figure B-1. For the landing analysis this curve was approximated by a number of straight line segments as indicated in this figure.

Determination of the strut load resulting from strut stroking for this typical load stroke curve, is as follows. Assuming initial stroking in the compressive direction, the strut load increases linearly with stroke to point 1, Figure B-1, at which time the first "corner" is reached. The slope of the second portion of the curve then defines the linear increase in load with stroke. The load continues to follow the load stroke curve until the direction of stroke reverses, such as point 2. With continued decrease in strut stroke, one of the following load stroke sequences is possible, Figure B-2.

1. Elastic unloading through point 3, Figure B-2A, at which time the load becomes tension. Continued decrease in the magnitude of strut stroke results in the load moving through point 4 on to a point such as indicated at 5. Note that past point 3, the strut load is governed by the input tension load stroke curve with an effective zero stroke point located at point 3.

2. If, following the sequence of stroking discussed above, the stroke again reverses direction at point 5, Figure B-2B, the load decreases in tension to zero, point 6, and then increases in compression. Additional compressive stroke results in loads defined by the original compressive load-stroke relationship with an effective point of zero stroke at point 6.

3. If during the initial unloading discussed in paragraph 1, the stroke reversed a second time at point 7, Figure B-2C, before reaching the first tension "corner," point 4, a different loading sequence would result. With further increase in compressive stroke from point 7, the load would return to point 2, the initial unloading point, and then continue to follow the original load stroke curve as indicated to point 8.

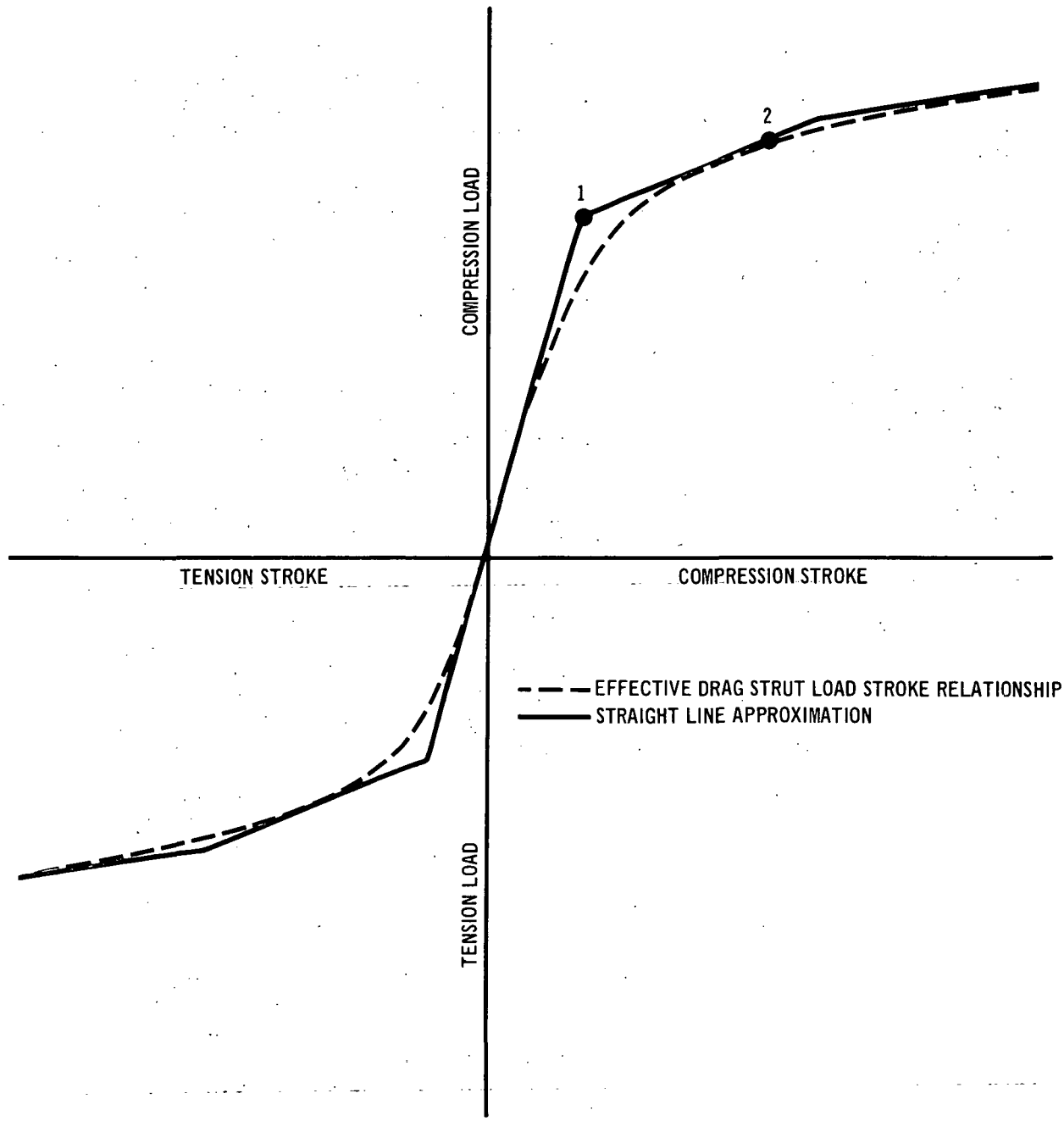

FIGURE B–1 EFFECTIVE DRAG STRUT LOAD STROKE RELATIONSHIP FOR VIKING LANDER

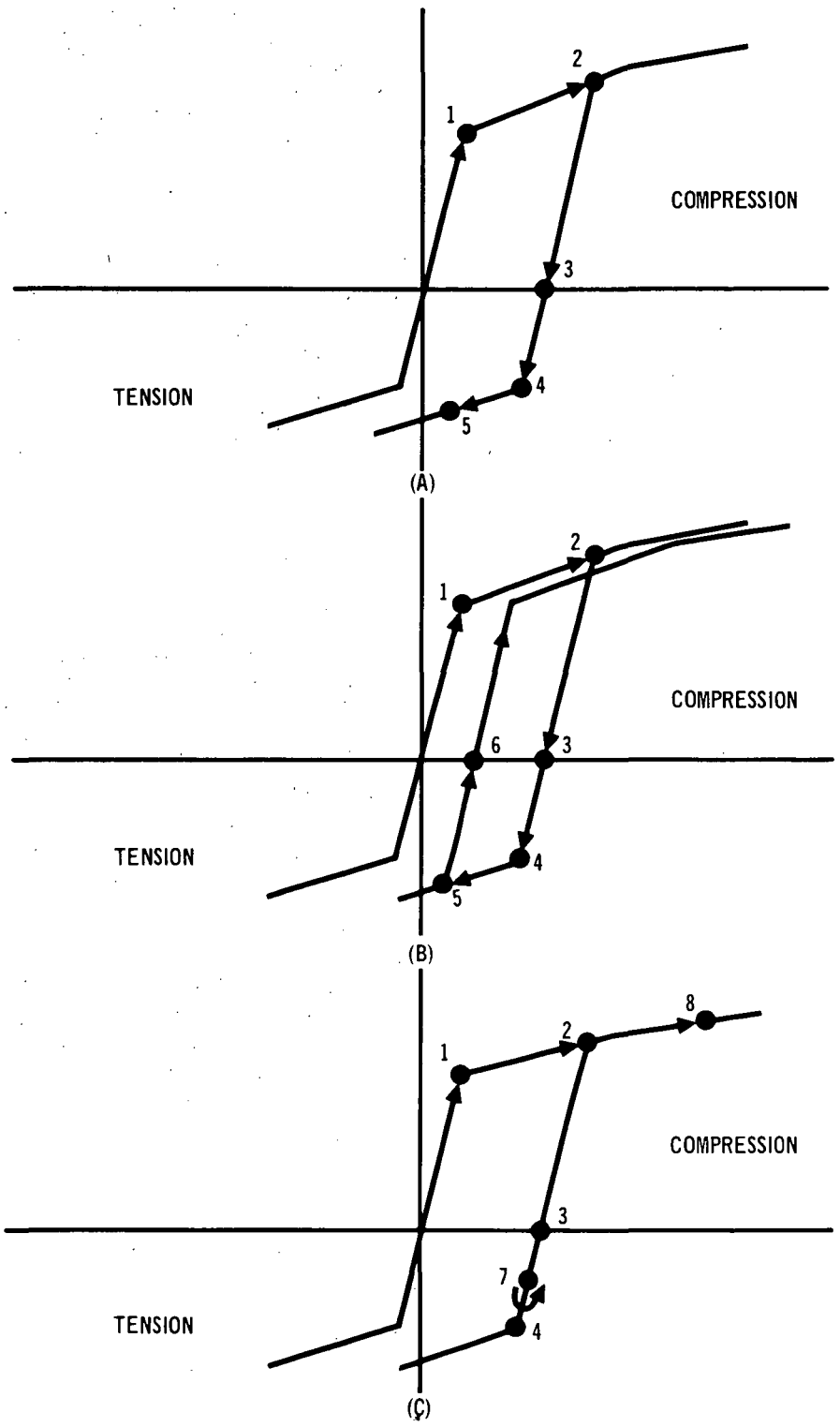

FIGURE B–2 POSSIBLE UNLOADING SEQUENCES OF EFFECTIVE VIKING LANDER DRAG STRUT

NATIONAL AERONAUTICS AND SPACE ADMINISTRATION
WASHINGTON, D.C. 20546

OFFICIAL BUSINESS

FIRST CLASS MAIL

POSTAGE AND FEES PAID
NATIONAL AERONAUTICS AND
SPACE ADMINISTRATION

POSTMASTER: If Undeliverable (Section 158
Postal Manual) Do Not Return

"The aeronautical and space activities of the United States shall be conducted so as to contribute . . . to the expansion of human knowledge of phenomena in the atmosphere and space. The Administration shall provide for the widest practicable and appropriate dissemination of information concerning its activities and the results thereof."

—National Aeronautics and Space Act of 1958

NASA SCIENTIFIC AND TECHNICAL PUBLICATIONS

TECHNICAL REPORTS: Scientific and technical information considered important, complete, and a lasting contribution to existing knowledge.

TECHNICAL NOTES: Information less broad in scope but nevertheless of importance as a contribution to existing knowledge.

TECHNICAL MEMORANDUMS: Information receiving limited distribution because of preliminary data, security classification, or other reasons.

CONTRACTOR REPORTS: Scientific and technical information generated under a NASA contract or grant and considered an important contribution to existing knowledge.

TECHNICAL TRANSLATIONS: Information published in a foreign language considered to merit NASA distribution in English.

SPECIAL PUBLICATIONS: Information derived from or of value to NASA activities. Publications include conference proceedings, monographs, data compilations, handbooks, sourcebooks, and special bibliographies.

TECHNOLOGY UTILIZATION PUBLICATIONS: Information on technology used by NASA that may be of particular interest in commercial and other non-aerospace applications. Publications include Tech Briefs, Technology Utilization Reports and Technology Surveys.

Details on the availability of these publications may be obtained from:

SCIENTIFIC AND TECHNICAL INFORMATION DIVISION

NATIONAL AERONAUTICS AND SPACE ADMINISTRATION

Washington, D. C. 20546